NeuroImage xxx (2017) 1–18

Contents lists available at ScienceDirect

NeuroImage

journal homepage: www.elsevier.com/locate/neuroimage

Functional networks and network perturbations in rodents

Kai-Hsiang Chuang [a,b,*], Fatima A. Nasrallah [a]

[a] Queensland Brain Institute, The University of Queensland, Brisbane, QLD 4072, Australia
[b] Centre for Advanced Imaging, The University of Queensland, Brisbane, QLD 4072, Australia

ARTICLE INFO

Keywords:
Resting state network
Functional MRI
Functional connectivity
Brain connectome
Translational research

ABSTRACT

Synchronous low-frequency oscillation in the resting human brain has been found to form networks of functionally associated areas and hence has been widely used to map the functional connectivity of the brain using techniques such as resting-state functional MRI (rsfMRI). Interestingly, similar resting-state networks can also be detected in the anesthetized rodent brain, including the default mode-like network. This opens up opportunities for understanding the neurophysiological basis of the rsfMRI signal, the behavioral relevance of the network characteristics, connectomic deficits in diseases and treatment effects on brain connectivity using rodents, particularly transgenic mouse models. In this review, we will provide an overview on the resting-state networks in the rat and mouse brains, the effects of pharmacological agents, brain stimulation, structural connectivity, genetics on these networks, neuroplasticity after behavioral training and applications in models of neurological disease and psychiatric disorders. The influence of anesthesia, strain difference, and physiological variation on the rsfMRI-based connectivity measure will be discussed.

1. Introduction

Infra-slow (<0.1 Hz) oscillation in the resting (task-free) state reveals several large-scale resting-state networks (RSNs) that not only implicate the intrinsic functional organization of the brain but also present network plasticity or dysfunction in mental or pathological processes. However, with the neural basis and function of these RSNs remaining unclear, it is difficult to associate macroscopic observations with underlying neurophysiological, axonal, synaptic, and neuropathological changes. Animal models provide a powerful way to understand the neural basis of brain structure and function, pathological mechanisms of disorders, and therapeutic effects. Rodents, particularly transgenic mice, are the major animal models for brain diseases. Therefore, imaging RSNs in rodent brains is an important step in linking the findings of human research to underlying cellular and molecular mechanisms.

Despite the technical challenge (see (Pan et al., 2015) for a detailed review) and differences in neuroanatomical and functional organization between species (van den Heuvel et al., 2016), it has been demonstrated that similar RSNs, such as the bilateral connectivity in sensory and motor networks, can be consistently identified in the anesthetized rat (Biswal and Kannurpatti, 2009; Majeed et al., 2009; Pawela et al., 2008; Zhao et al., 2008), awake rat (Becerra et al., 2011; Liang et al., 2011; Upadhyay et al., 2011), and, more recently, anesthetized mouse (Grandjean et al., 2014a; Nasrallah et al., 2014c; Sforazzini et al., 2014b). Particularly, default mode (DMN)-like network has been found in both the rat (Lu et al., 2012) and mouse brain (Sforazzini et al., 2014b), indicating the evolutionally preservation of this large-scale network. Furthermore, RSNs in rodents can be detected not only by blood oxygenation level dependent (BOLD) resting-state functional MRI (rsfMRI) but also by alternative or invasive methods of varying signal source and spatiotemporal resolution, such as arterial spin labeling perfusion fMRI (Nasrallah et al., 2012a, 2012b), contrast enhanced cerebral blood volume (CBV) fMRI (Sforazzini et al., 2014b), optical intrinsic signal imaging of hemoglobin level (White et al., 2011), functional ultrasound imaging of cerebral blood flow (Osmanski et al., 2014), laser speckle imaging of blood flow and hemoglobin concentration (Bergonzi et al., 2015), and fluorescence imaging of voltage-sensitive dyes (Chan et al., 2015) or calcium indicators (Ma et al., 2016a; Matsui et al., 2016). Together with electrophysiological, histological, genetic and other techniques for characterizing cellular and molecular changes, rodent models offer significant potential to understand and validate the neurophysiological mechanisms of the rsfMRI signal, the behavioral relevance of the network characteristics, the connectomic signatures and mechanisms of diseases, and the effects of treatment on brain connectivity. In this review, we will focus on the findings obtained with rsfMRI and start by highlighting the organization of RSNs in the rodent brain and the influence of different

* Corresponding author. Queensland Brain Institute and Centre for Advanced Imaging, The University of Queensland Brisbane, Queensland 4072, Australia.
E-mail address: kaichuang@gmail.com (K.-H. Chuang).

https://doi.org/10.1016/j.neuroimage.2017.09.038
Received 11 August 2017; Received in revised form 15 September 2017; Accepted 19 September 2017
Available online xxxx
1053-8119/

anesthesia. We will further discuss the perturbation of networks by various manipulations, including neuro-pharmaceuticals, behavior, brain stimulation, structural connectivity and genetics/strain, and the translational relevance of disease models. Technical considerations regarding animal physiology and post-processing will also be discussed.

2. Resting-state network of the rodent brain

2.1. Organization and characteristics

Three kinds of functional connectivity (FC) patterns have been consistently identified in the sedated, anesthetized and awake rat brain (Fig. 1):

1) **Bilaterally symmetric connectivity within functional modules**. This includes the primary and secondary somatosensory, motor, and visual cortices, hippocampus and subcortical areas, such as the caudate putamen, thalamus, superior colliculus, and hypothalamus (Hutchison et al., 2010; Majeed et al., 2009; Pawela et al., 2008; Zhao et al., 2008).
2) **Anteroposterior connectivity along the midline**. This is found between the cingulate and retrosplenial cortices (Hutchison et al., 2010; Jonckers et al., 2011).
3) **Large-scale cross-modular connectivity**. The DMN-like connectivity is of this type. It was initially only detected in the well-habituated awake rat brain, and comprised the cingulate (homologous to the human anterior cingulate cortex), retrosplenial (homologous to the human posterior cingulate cortex) and parietal cortices and hippocampus (Upadhyay et al., 2011). However, with a more stable anesthesia regimen that combined medetomidine and light isoflurane, a more extensive network consisting of the orbital cortex (homologous to the human orbital frontal cortex), prelimbic and cingulate cortex, retrosplenial cortex, posterior parietal cortex, auditory/temporal associated cortex, and dorsal hippocampus could be detected (Lu et al., 2012).

With the success of rsfMRI of the rat brain, attempts have been made to detect similar RSNs in the mouse brain. However, initial studies only detected unilateral connectivity (Jonckers et al., 2011), possibly due to sub-optimal anesthesia and the physiological state of the mouse which can be more difficult to maintain than that of the rat. With improved anesthetic and physiological control, a few groups have recently succeeded in demonstrating stereotypic bilateral connectivity in the somatosensory, motor, auditory and visual cortices, as well as in the caudate putamen, thalamus, hippocampus and cerebellum, and anteroposterior connectivity in the prefrontal, cingulate and retrosplenial cortices, similar to the patterns reported in the rat brain (Fig. 1B) (Grandjean et al., 2014a; Nasrallah et al., 2014c; Sforazzini et al., 2014b; Zerbi et al., 2015). Furthermore, DMN-like connectivity and another large-scale network composed of the ventrolateral striatum, nucleus accumbens, anterior insular and cingulate cortex, similar to the salience network in humans, were identified (Sforazzini et al., 2014b).

Another similar feature of rodent RSNs is their anti-correlation. Anti-correlated networks have been reported in humans, particularly between the task-positive network (including the intraparietal sulci, supplementary motor area, precentral gyrus and insula) and the task-negative network (e.g., DMN) (Fox et al., 2005). Earlier studies in rats did not observe anti-correlation which could be partly due to the effects of anesthesia (Liang et al., 2012a). Nonetheless, anti-correlated networks similar to those in humans have recently been identified in medetomidine-sedated rats (Schwarz et al., 2013) and in propofol- or halothane-anesthetized mice (Grandjean et al., 2014a; Sforazzini et al., 2014b). Furthermore, another study reported that aged rats exhibit a change in anti-correlation between the retrosplenial cortex (part of rodent DMN) and the fronto-insular cortex that may be related to their memory performance (Ash et al., 2016).

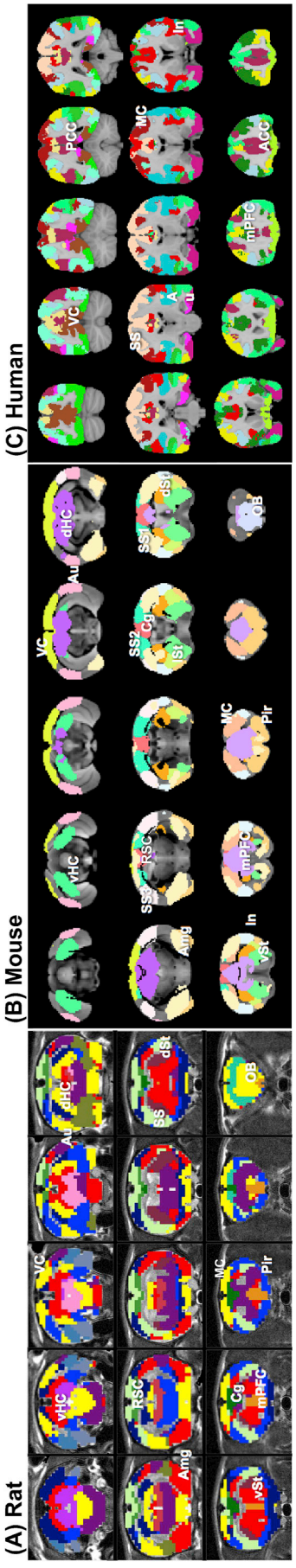

Fig. 1. RSNs of the rodent and human brain. (**A**) 40 functional parcels in the awake rat brain with adjacent parcels having different colors (adapted from Ma et al., 2016b). (**B**) 17 functional networks in the anesthetized mouse with different colors representing different networks (adapted and replotted from Zerbi et al., 2015). (**C**) 17 functional parcels in the human cerebral cortex (adapted from Yeo et al., 2011). The labels indicate similar networks that can be identified among species. ACC: anterior cingulate (equivalent to Cg in rodents); Amg: amygdala; Au: auditory cortex; Cg: cingulate cortex (equivalent to ACC in humans); dHC: dorsal hippocampus; dSt: dorsal striatum; In: insular cortex; lSt: lateral striatum; mPFC: medial prefrontal cortex; MC: motor cortex; PCC: posterior cingulate (equivalent to RSC in rodents); Pir: piriform cortex; RSC: retrosplenial cortex (equivalent to PCC in humans); SS1,2,3: somatosensory area 1,2,3; VC: visual cortex; vHC: ventral hippocampus. From top to bottom: posterior to anterior.

Overall, apart from the second type of RSN that is well-separated in humans (Fig. 1C), the other connectivity patterns are highly similar to those which have been observed in awake humans, suggesting a conservation of RSNs across species and the potential of RSNs as translatable biomarkers. In particular, this provides the opportunity to use widely available transgenic models and invasive tools to understand the neurophysiological and pathological mechanisms and functional roles of RSNs.

2.2. Verification of functional relevance

Given that topological similarity does not necessary imply functional similarity, the first question to answer is whether the functions of the rodent RSNs, particularly the DMN-like network, are similar to those in humans. The human DMN is characterized by regions that are hyperactive at rest but suppressed during attention- and goal-oriented tasks. It has been suggested that the DMN is involved in internal processes, such as self-referential tasks and memory consolidation, and is hampered in diseases like dementia (Raichle, 2015). By measuring brain oxygenation in awake behaving rat, it was found that task performance reduced the FC between nodes in the DMN-like network, but not between the motor and somatosensory cortices, showing similar characteristics to those of the human DMN that is more active at rest but suppressed during cognitively demanding tasks (Li et al., 2015a). In an attempt to elucidate its involvement in memory processes, we demonstrated that connectivity within the rat DMN is increased after maze learning but decreased one week later, suggesting that the rodent DMN may be involved in early memory consolidation (Fig. 2) (Nasrallah et al., 2016a). Other groups further identified sub-network modules in the rat DMN that display age- and behavior-related decline (Ash et al., 2016; Hsu et al., 2016). Together, these findings support the functional relevance of the rodent DMN and the use of rodents as translatable models for studying higher-order functional changes.

2.3. Functional parcellation and modules of the brain

To understand the functional segregation and organization of RSN modules and their correspondence with the neuroanatomy of the brain, functional parcellation based on rsfMRI has been extensively studied in humans. Similar functional parcellation of the sedated mouse brain was explored using independent component analysis (ICA) (Mechling et al., 2014), voxel-wise correlation (Liska et al., 2015) or wavelet-based clustering of spectral dynamics (Medda et al., 2016). By separating the rsfMRI data into 100 independent components, more than 90 functional parcels that match known cortical and subcortical structures could be identified, which could then be grouped into 5 bilaterally symmetric network modules from medetomidine sedated mouse brain: basal ganglia, sensory-motor and limbic, anterior cingulate, visual processing and memory, and hypothalamus (Mechling et al., 2014). With voxel-wise analysis, six highly interconnected modules could be identified in halothane anesthetized mouse brain: DMN, lateral cortical network (including the somatosensory and motor cortices), hippocampus, basal forebrain, ventral midbrain (including the amygdala and hypothalamus), and thalamus (Liska et al., 2015). Despite the use of different anesthesia and parcellation methods, similar functional networks could be identified, indicating high reproducibility. However, no network in the dorsal midbrain and brainstem was differentiated, likely due to the effect of anesthesia.

Recently, using a voxel-wise correlation analysis in the awake rat brain, fine-grain sub-networks was identified that were highly consistent with anatomical areas in the prefrontal, motor, cingulate, somatosensory, olfactory, auditory and visual cortices, as well as in the amygdala, striatum, hippocampus, thalamus, hypothalamus, midbrain and brainstem (Fig. 1A) (Ma et al., 2016b). These networks were highly symmetric and the homogeneity of the rsfMRI signal in the functional parcel was greater than that in the anatomical parcel, suggesting that using anatomical structure to define functional regions for rsfMRI analysis may not be the optimal approach. Similar work will be needed in the awake mouse to define the functional parcels suitable for FC analysis.

3. Effects of anesthesia on functional networks

Anesthesia has been used in most rodent rsfMRI studies to minimize stress and movement of the animal. Although anesthesia is known to elicit complicated effects on neural, metabolic and hemodynamic responses (see Gao et al., 2016; Masamoto and Kanno, 2012; for review), studies have demonstrated that RSNs are highly reproducible and consistent across different anesthesia regimens at optimal dose. The fact that FC can be altered by anesthesia also makes rsfMRI a powerful tool to understand the mechanism of anesthesia (Nallasamy and Tsao, 2011).

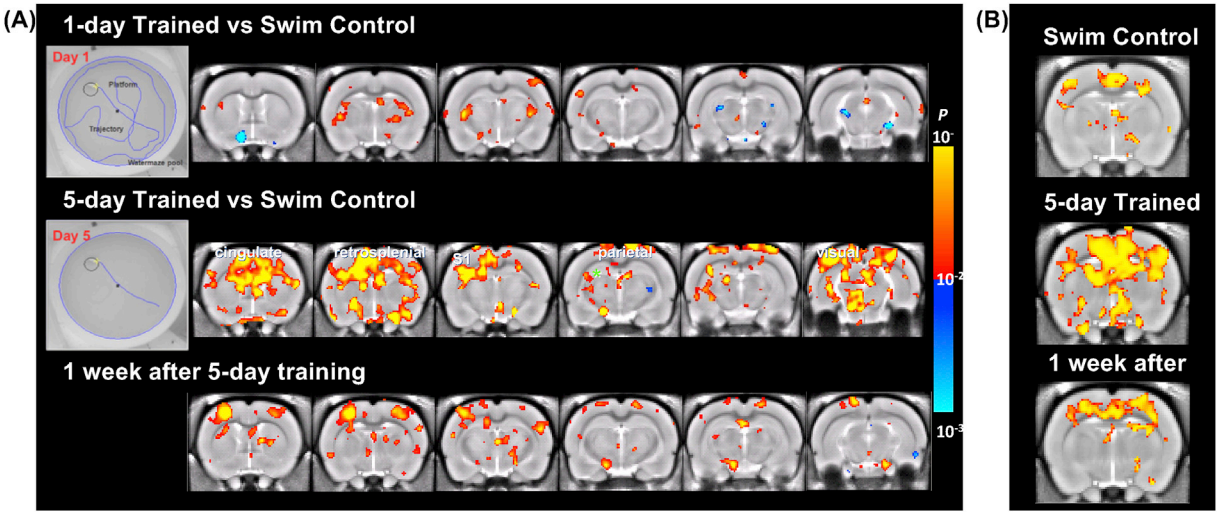

Fig. 2. Learning induces long-lasting plasticity in the RSN. To determine the RSN changes caused by learning, two groups of rats either underwent 5 days of spatial learning to locate a hidden platform in a Morris water maze or swam for the same period of time without the hidden platform. One day and 7 days after finished the training, rsfMRI was conducted under medetomidine sedation. Seed-based correlation analysis was performed and the network difference between the maze learning group and the swim control group was tested by two-tailed *t*-test ($p < 0.01$, FDR corrected). (**A**) Extensively enhanced connectivity with the hippocampal CA3 region was observed after 5 days of training in a Morris water maze. The connectivity was sustained 1 week after the training but reorganized toward cortical areas. (**B**) The DMN-like network showed transiently increased connectivity but returned to baseline after a week. Adapted from Nasrallah et al. (2016a,b).

The neural effect of anesthesia mainly arises from the sites of anesthetic action, the associated downstream neural activities, and the regions related to unconsciousness and arousal. For example, as most anesthetics bind to the γ-amino butyric acid (GABA) receptors, FC within and between regions of high GABAergic receptor density, such as the thalamus and caudate putamen, is generally weaker. The thalamocortical, frontoparietal and DMN connectivity, which are important for integration of information, attention and consciousness, are affected under anesthesia (Hudetz, 2012; Nallasamy and Tsao, 2011). Given that some forms of anesthesia also have an analgesic effect, the connectivity in the pain pathway, which involves regions like somatosensory and cingulate cortices and the thalamus, would also be affected. Besides the neural effect, anesthesia typically affects cardiopulmonary and vascular functions, leading to systemic changes in blood oxygenation, basal cerebral blood flow (CBF), vascular reactivity and, ultimately, neurovascular coupling (see (Masamoto and Kanno, 2012) for review). Therefore, these factors should be considered in any experimental design and interpretation of results. As these effects are typically dosage dependent, an optimized dose will allow measurement of spontaneous neural oscillation with minimal hemodynamic and physiological confounds (Paasonen et al., 2016; Schroeter et al., 2014). In the following section, the effects of commonly used anesthetics for rodent rsfMRI are summarized and compared with the results obtained in non-anesthetized animals (see the summary in Table 1).

3.1. α-chloralose

α-chloralose has been widely used in rodent fMRI due to its minimal impact on neuro-metabolic coupling (Ueki et al., 1992). It can potentiate GABAergic transmission without affecting glutamatergic or cholinergic transmission (Wang et al., 2008), and allows measurement of FC with strong strength and good localization, although the connectivity in the caudate putamen, where the $GABA_A$ receptor density is high, is much lower (Paasonen et al., 2016; Williams et al., 2010). α-chloralose has strong dosage-dependent effects on evoked activation and interhemispheric coherence such that bilateral BOLD signal correlation and delta band coherence of local field potential (LFP) are attenuated at high dose (Lu et al., 2007). As this anesthesia can cause acidosis, the arterial blood pCO_2 level could be increased and alter the CBF and BOLD signal during prolonged measurement (Low et al., 2016a). Dissolving α-chloralose in polyethylene glycol may avoid acidosis and hence may help to minimize its physiological impact (Jonckers et al., 2014).

3.2. Isoflurane

As isoflurane is a quick, easy and safe way to anesthetize animals and ensure good recovery, it has been an attractive choice in fMRI and longitudinal studies. Isoflurane acts on multiple systems, including the glutamatergic and GABAergic systems, and has a strong vasodilatory effect that alters CBF and neurovascular coupling in a dosage-dependent manner (Masamoto et al., 2009). At a low dose, such as 1–1.5%, a strong focal connectivity pattern can be obtained, although with suppressed thalamocortical connectivity (Bukhari et al., 2017; Grandjean et al., 2014a; Hutchison et al., 2014; Nasrallah et al., 2014a). Isoflurane has strong dosage-dependent effect on RSNs with reduced or complete loss of bilateral FC at high dose due to its suppression of both spontaneous activity and synchrony (Nasrallah et al., 2014a; Wang et al., 2011). A major complication in terms of RSNs is that isoflurane could induce burst-suppression activity across the brain at mid-to-high dose (e.g., >1.8% in rats) and hence could lead to a strong global correlation (Kalthoff et al., 2013; Liu et al., 2011; Liu et al., 2013b; Williams et al., 2010). Therefore, the dose should be kept to the minimal level. As physiology and motion are more difficult to control under a low dose of isoflurane, the use of mechanical ventilation together with a paralyzing agent would be preferable to minimize the variation.

3.3. Medetomidine/dexmedetomidine

Unlike most anesthesia that acts on GABAergic and/or glutamatergic systems, medetomidine is a sedative that specifically agonizes the α2-adrenergic receptor. Dexmedetomidine is the active enantiomer of medetomidine and has twice the potency; consequently, the dosage is typically half that of medetomidine. Both agents cause bradycardia and act as vasoconstrictors that increase blood pressure and reduce CBF. Given that they have less impact on neural activity and neurovascular coupling than other general anesthetics and are easily reversible by an antagonist, atipamezole, to allow quick recovery and facilitate longitudinal studies, they have been widely used in task and resting fMRI studies

Table 1
Summary of anesthesia effects.

Anesthesia/Sedative	Neural effect	Vascular effect	Functional connectivity	Species and Reference
α-chloralose	• GABAergic	Minimal but increases CBF due to acidosis	• Reduces bilateral FC dose dependently	• Rat (Lu et al., 2007; Williams et al., 2010) • Mouse (Jonckers et al., 2014)
Isoflurane	• Glutamatergic, GABAergic • Burst-suppression activity	Vasodilation	• Increases FC at mid dose due to burst-suppression activity. • Abolishes FC at high dose.	• Rat (Bukhari et al., 2017; Hutchison et al., 2014; Kalthoff et al., 2013; Liu et al., 2011; Liu et al., 2013b; Nasrallah et al., 2014a; Williams et al., 2010) • Mouse (Grandjean et al., 2014a; Jonckers et al., 2014)
Medetomidine	• Adrenergic • Sedative • Potential epileptic effect	Vasoconstriction without affecting neurovascular coupling	• Reduces bilateral FC dose, region and time dependently	• Rat (Nasrallah et al., 2014a, 2012b; Pawela et al., 2008; Williams et al., 2010; Zhao et al., 2008) • Mouse (Grandjean et al., 2014a; Nasrallah et al., 2014c)
Medetomidine + isoflurane	• Stable sedation • Suppresses potential epileptic effect	Decreases pCO_2 after a long period	• Stable FC for up to 3 h	• Rat (Brynildsen et al., 2017; Fukuda et al., 2013; Lu et al., 2012) • Mouse (Grandjean et al., 2014a)
Propofol	• GABAergic • Hypnotic at low dose and deep anesthesia at high dose	Minimal but reduces CBF at high dose	• Cortical FC reduced with dose • Regions related to arousal do not change with dose	• Rat (Liu et al., 2013a) • Mouse (Grandjean et al., 2014a)
Urethane	• Glutamatergic, GABAergic • Induces sleep-like states	Minimal but could induce slow hemodynamic oscillation	• Reduces bilateral FC with dose • FC dependent on fast or slow wave state	• Rat (Wilson et al., 2011; Zhurakovskaya et al., 2016) • Mouse (Grandjean et al., 2014a; Jonckers et al., 2014)
Awake	• Potential chronic stress • Pain sensitivity	Minimal	• Generally stronger FC • Stronger anti-correlation	• Rat (Becerra et al., 2011; Liang et al., 2012a, 2011) • Mouse (Jonckers et al., 2014)

in rodents (Nasrallah et al., 2014a; Weber et al., 2006; Williams et al., 2010; Zhao et al., 2008). Strong and focal RSNs can be detected at low dose, but the connectivity reduces dosage- and duration-dependently, particularly in regions with high α2 receptor density, such as the thalamus, whereas regions with low receptor density, such as the caudate putamen, remain relatively unaffected (Grandjean et al., 2014a; Nasrallah et al., 2014a, 2014c, 2012b). Nonetheless, unlike with isoflurane, the thalamocortical connectivity is preserved (Bukhari et al., 2017). Interestingly, increasing the dosage has no effect on the neurovascular coupling, evoked activation or fluctuation amplitude, but rather reduces the synchrony, especially the γ oscillation, suggesting that sedation is caused by a loss of functional integration (Nasrallah et al., 2014a). A limitation of medetomidine is the restrictive sedative duration (Nasrallah et al., 2014c; Weber et al., 2006). Although increasing the dose could extend the duration, the FC strength changes (Pawela et al., 2009). Prolonged measurement could be achieved with a higher dose, but the FC gradually decreases, probably due to excess receptor binding (Nasrallah et al., 2014c), and there is a tendency towards epileptic activity after long periods of sedation (Fukuda et al., 2013). However, combining medetomidine with a very low dose of isoflurane has proven a reliable way to extend the sedation period while avoiding the neurophysiological impacts (see below).

3.4. Medetomidine + isoflurane

A low level of isoflurane (<0.5%) together with a low dose of medetomidine infusion is likely to be the most robust anesthesia for detecting strong bilateral FC, the DMN and even anti-correlation in the rodent brain (Grandjean et al., 2014a; Lu et al., 2012). This combination has the advantage of suppressing the potential epileptic effects of long duration medetomidine without altering the evoked potential (Fukuda et al., 2013). In addition, it may help to overcome the strain-dependent susceptibility to medetomidine and provide more robust sedation across strains. It also allows measurement of neuronal and hemodynamic responses over an extended period (~3 h) compared to using medetomidine alone. Nonetheless, gradually increased respiration rate and decreased pCO_2 eventually compromise the hemodynamic response for experiments longer than 3 h (Brynildsen et al., 2017; Fukuda et al., 2013).

3.5. Propofol

Propofol is a $GABA_A$ receptor agonist that has the advantage of not attenuating BOLD activation even at high dose (Liu et al., 2013c; Schroeter et al., 2014), indicating well-preserved neurovascular coupling. It has minimal vascular effects although CBF could be reduced at high dose (Liu et al., 2013a). Interestingly, propofol can be used to induce hypnotic sedation through to deep anesthesia for surgery as the dosage increases and produces strong dosage-dependent changes in RSNs. Therefore, it has proven an attractive anesthetic for studying the loss of consciousness (Barttfeld et al., 2015). With increased dose, cortical connectivity in the motor cortex and DMN decreases while thalamic and hypothalamic connectivity, which control arousal and the conscious state, remains stable; in some subcortical areas, such as the hippocampus and caudate putamen, connectivity is reduced but rebounds at a higher dose, likely because of increased burst-suppression activity (Liu et al., 2013a). Similar to isoflurane and α-chloralose, which also bind to the $GABA_A$ receptor, the thalamic connectivity is weak even at very low doses. Greater anti-correlation can be observed under propofol compared to medetomidine although the mechanism is not clear (Grandjean et al., 2014a).

3.6. Urethane

Urethane acts on multiple neurotransmitter systems, including the $GABA_A$ and N-methyl-D-aspartate (NMDA) receptors (Hara and Harris, 2002). It has been widely used in rodent fMRI and electrophysiology studies due to its minimal impact on systemic hemodynamics and the cardiovascular system (Janssen et al., 2004). In the resting state, urethane shows dosage-dependent depression of bilateral connectivity and loss of spatial specificity (Grandjean et al., 2014a; Jonckers et al., 2014). Most interestingly, urethane can induce sleep-like states, including rapid eye movement (fast wave) and non-rapid eye movement (slow wave) states, and hence exhibits different FC strengths/patterns that depend on the sleep state (Wilson et al., 2011; Zhurakovskaya et al., 2016). Therefore, it could be used to investigate RSN dynamics in sleep. As the state changes dynamically under the same anesthesia dose, electroencephalogram recording or, alternatively, respiration rate is needed to determine the exact brain state for which the RSN is measured (Wilson et al., 2011). It should be noted that urethane could have a vascular effect with broad and slow hemodynamic oscillation that does not correlate with local excitatory neural oscillation in the resting state (Ma et al., 2016a).

3.7. Awake

A few studies have explored the RSN in awake restrained rodents. As the neural and hemodynamic activities are not attenuated by anesthesia, the spontaneous activity amplitude and FC strength are generally greater. Furthermore, more long-range connections can be detected in awake compared to isoflurane-anesthetized rats, particularly in the striatum, pallidum, thalamus, and cortex, while the FC in hippocampus, amygdala, and hypothalamus are reduced in awake rats (Chang et al., 2016; Liang et al., 2012b, 2011). In particular, thalamocortical connectivity, which is difficult to detect under isoflurane, can be better resolved in awake rodents (Liang et al., 2013b). Anti-correlation, which is occasionally reported in anesthetized rodents, can also be detected easily in awake rodents (Liang et al., 2012a). Awake mouse rsfMRI has proven more challenging than that in rats, with recent attempts showing weak bilateral connectivity (Bergmann et al., 2016; Jonckers et al., 2014). As mice generally become stressed more easily than rats (Ellenbroek and Youn, 2016), improved restraint design (Chang et al., 2016), a shorter restrained period and more days for acclimation (Harris et al., 2015) would be needed to train them. Although acclimation to restraint inside the MRI scanner has been shown to reduce movement and stress, chronic stress may be induced after prolonged restraint and could result in elevated FC in certain networks, such as the somatosensory and visual cortices and the DMN (Henckens et al., 2015). In addition, the restraint training may also lead to a reduced response to pain (Low et al., 2016b), which could confound the RSN detected. Constantly received strong sensory inputs from the MRI scanner environment and the tendency to escape may also alter the spontaneous activity and RSN in awake condition.

3.8. Practical consideration

FC strength, network organization and the number of dynamic states could change not only with the anesthesia dose but also based on the route and timing of delivery (Hutchison et al., 2014; Liang et al., 2014b). In particular, using a single bolus injection rather than continuous delivery could lead to a variable depth of anesthesia, physiological state and FC depending on the pharmacokinetics and pharmacodynamics of the anesthetic. In a study comparing several anesthetics, stable FC over a 1-hour interval was only observed under continuously delivered anesthesia (Paasonen et al., 2016). Another study on the transition from deep to light anesthesia found drastically increased FC in the latter case (Bettinardi et al., 2015). Therefore, continuous delivery, which provides a more stable depth of anesthesia, is preferable to ensure more consistent and reproducible FC measurements, particularly over long periods for data averaging or to detect drug effects (Paasonen et al., 2016). Furthermore, FC strength could be affected by the duration under general anesthesia (typically isoflurane) (Magnuson et al., 2014a). Therefore, the preparation duration should be minimized and standardized.

Anesthesia may affect the spectral distribution of spontaneous activity. Whereas most human studies focus on a frequency range below 0.1 Hz, several rodent studies have shown that resting-state activity could peak at higher frequencies depending on the type of anesthesia. For example, the resting BOLD signal under medetomidine and its mixture with isoflurane presents high spectral power between 0.1 and 0.2 Hz whereas the BOLD signal under isoflurane is mostly below 0.1 Hz (Grandjean et al., 2014a; Pan et al., 2013). The spectral component could also change with the duration of anesthesia. For example, high frequency peaks start to emerge after a long period of medetomidine sedation (Magnuson et al., 2014a). Given that the high frequency oscillation could contain more dynamic characteristics of the FC or even disease-related features, as shown by recent studies in human patients (Calhoun et al., 2012), more rigorous investigations incorporating high temporo-spectral information are needed.

Finally, it should be noted that the anesthetic effect could be animal species, strain, gender, age and disease state dependent. For example, the anesthetic dose is generally lower in neonatal and aged animals (Chemali et al., 2015; Colonnese et al., 2008). It has been shown that the duration of anesthesia in albino rats is generally longer than that in the pigmented ones (Avsaroglu et al., 2007). BALB/c and I/LnJ mice have lower depth of anesthesia than C57BL/6 mice under isoflurane, which could affect the quantitative measure of evoked and resting BOLD amplitudes (Schroeter et al., 2017). Whereas medetomidine can sedate C57BL/6 mice well, it is not as effective in BTBR T + tf/J or CD1 mice, which may reflect strain differences in the affinity and density of α2-adrenergic receptors (Petrinovic et al., 2016). Our preliminary data have also shown that FVB mice cannot be sedated using medetomidine, even at very high doses. Sprague Dawley and Wistar rats are more sensitive to medetomidine than C57BL/6 mice, with bilateral FC abolished at 0.3 mg/kg/h in rats compared to >0.6 mg/kg/h in mice (Nasrallah et al., 2014c, 2012b; Pawela et al., 2009). Therefore, the equivalent dose should be determined when comparing across ages, between a disease model and its wild-type control, or between strains.

4. Pharmacological effects on functional networks

Pharmacological MRI (phMRI) has been used to map the neural activation induced by a drug challenge in order to understand the pharmacodynamics in the brain (see (Jonckers et al., 2015) for review). Similarly, a change in FC could also be a pharamcodynamic readout for evaluating the efficacy of drug treatment. Furthermore, using drugs that target specific receptors could help to delineate the neural correlate of FC in relation to the underlying neurotransmission, receptor system, pathway or functional deficit. Various studies have shown that rsfMRI is sensitive enough to detect drug modulation of RSNs. In the following section, the effect of drugs that target the major neurotransmission systems are discussed. Although RSNs detected under drug infusion are strictly no longer resting state, the same term will be used in the following discussion for consistency. In addition, most studies are conducted with acute injection of drugs. Studies involving chronic or sub-chronic drug delivery are highlighted.

4.1. Glutamatergic

Glutamate is the primary excitatory neural transmitter and has been implicated in a broad range of neurological and psychiatric disorders. Most studies have focused on the effects of NMDA receptor antagonists, such as ketamine and memantine, on prefrontal-hippocampal connections in psychosis and memory. Acute injection of ketamine induces a dosage-dependent increase in FC in the prefrontal cortex and its connectivity with the hippocampus, supporting its role on disinhibition (Gass et al., 2014b). On the other hand, sub-chronic injection of memantine for 5 days reduces BOLD activation and the prefrontal-hippocampal FC, consistent with the reduction found in schizophrenia (Sekar et al., 2013). Our preliminary study with chronic low-dose memantine treatment over 6 months also found a decrease in FC and the amplitude of low frequency fluctuation without affecting BOLD activation. This difference may be due to time- and dose-dependent effects or actions on other neurotransmitter systems by NMDA ligands themselves at high dose (Kapur and Seeman, 2002). For example, FC among the prefrontal cortex, hippocampus and other cortical areas is increased at very low dose but decreased at higher doses of phencyclidine (PCP), a NMDA antagonist, together with impaired social interaction similar to that observed in schizophrenia (Paasonen et al., 2017). A potential confound in these studies is the interaction with anesthesia because several anesthetics, such as halothane and isoflurane, also act on NMDA receptors (Gozzi et al., 2008; Hodkinson et al., 2012). To eliminate this confound, a study using oxygen amperometry in freely moving rats found that ketamine induces an increase in FC between the medial prefrontal cortex and striatum, consistent with the rsfMRI results obtained in anesthetized rodents (Li et al., 2014). Cerebrovascular effects could also play a role. A comparison between NMDA and α-amino-3--hydroxy-5-methyl-4-isoxazolepropionic acid (AMPA) receptor antagonistic effects on the BOLD signal and electrophysiological activation revealed that although both forms of antagonism reduced evoked activity, the NMDA receptor mediated a stronger vascular response (Gsell et al., 2006).

4.2. GABAergic

GABA is the major inhibitory neurotransmitter and is involved in wakefulness, neuroplasticity, neurological and mental disorders and therapeutics. Several human studies have shown that the GABA level correlates with evoked activation and FC strength (Hu et al., 2013; Muthukumaraswamy et al., 2009; Northoff et al., 2007). Although the effects of specific GABAergic ligands on RSNs have been lacking, we recently showed that antagonizing the $GABA_A$ receptor with bicuculline induced significant widespread enhancement of FC across the brain, in particular inter-network connectivity; however, this change in FC did not correlate with receptor distribution and hence may reflect downstream excitatory transmission (Nasrallah et al., 2017). The effects of GABAergic activity could also be derived from anesthetics that potentiate the GABAergic system, such as propofol, although propofol also acts on the endocannabinoid system. Isoflurane, the commonly used anesthetic for drug studies, also positively modulates the $GABA_A$ receptor while suppressing glutamatergic transmission. Therefore, the drug effect under anesthesia could involve other systems. Furthermore, GABA interneurons can control vascular tone independent of the evoked potential and neurovascular coupling (Cauli et al., 2004; Fergus and Lee, 1997) and hence may complicate the BOLD signal readout.

4.3. Adrenergic

The adrenergic system, a major neuromodulatory system that regulates arousal, attention, mood, learning, memory, and stress response, has been a drug target for diseases such as attention-deficit/hyperactivity disorder (ADHD) (Cinnamon Bidwell et al., 2010). The influence of the α2-adrenergic system on RSNs has been studied using its agonist and antagonist. The α2 agonist can increase FC whereas the antagonist has the opposite effect depending on the dosage and regional receptor density (Nasrallah et al., 2014b, 2012b). Under slow infusion of α2 agonist, regions with high receptor density show a decrease in FC much earlier and more significantly than regions with low receptor density. Furthermore, the α2 system modulates neural synchrony in particular without affecting neural activation, which has been suggested as a mechanism of the sedative effect of the agonist (Nasrallah et al., 2014a). Although adrenergic drugs are highly receptor specific, drug-anesthetic interactions could still occur as the adrenergic system modulates glutamatergic and GABAergic neurons (Bennett et al., 1998).

4.4. Cholinergic

Cholinergic signaling arises from several nuclei, particularly the

striatum and nucleus accumbens in the basal forebrain, can modulate neural excitability, synaptic plasticity and coordinated activity, and is involved in attention, learning and memory (Picciotto et al., 2012). Due to the prevalent use of acetylcholinesterase inhibitors, such as donepezil, in the treatment of Alzheimer's disease (AD), the influence of the cholinergic system on FC and cognitive functions have been studied in elderly humans and patients but not in young healthy subjects (Li et al., 2012). Injection of scopolamine, a muscarinic acetylcholine receptor (mAChR) antagonist, results in dosage-dependent reduction of BOLD signal intensity and FC within the DMN (Shah et al., 2016a). Furthermore, a broad reduction in inter-regional FC in the cortex, hippocampus and thalamus was found to correspond to impaired learning performance, which can be partially reversed by an agonist, milameline (Shah et al., 2015). Consistent with this, our preliminary study on enhancing cholinergic transmission with sub-chronic treatment with donepezil showed that striatal and hippocampal FC were increased and corresponded with better performance in a water maze. As cholinergic neurons innervate cerebral blood vessels and regulate CBF, the BOLD signal and even the behavioral performance may be changed by the vasoconstrictive effect of cholinergic antagonist (Kocsis et al., 2014). Another mAChR antagonist, methyl-scopolamine, which does not cross the blood-brain barrier was used to show that FC change is not due to vascular effects (Shah et al., 2015).

4.5. Dopaminergic

Dopamine is involved in reward, aversion, cognitive control and motor function. The nigrostriatal dopamine pathway that projects from the substantia nigra is crucial for motor function, and the mesolimbic and mesocortical dopamine pathways which arise from the ventral tegmental area are important for motivational function (Wise, 2004). Injection of haloperidol, a widely used antipsychotic and dopamine D2 antagonist, induces broad modulation of the downstream circuits, including reduced FC between the substantia nigra and regions in the ascending dopaminergic projections and increased FC between the habenula, an important relay center for the midbrain nuclei, and the striatum, which is consistent with the dyskinetic side effects (Gass et al., 2013). Due to its important role in psychosis, dopaminergic blockade has been used to assess the effects of other psychosis-inducing drugs, such as ketamine, on the dopamine system (Colon-Perez et al., 2016; Li et al., 2014).

4.6. Serotoninergic

Serotonin (5-HT), which is produced in the raphe nuclei and distributed across the brain, regulates mood, appetite and sleep and has been widely used as a drug target for the treatment of depression (Berger et al., 2009). Enhancing serotonin transmission with a 5-HT_{1A} agonist increases FC with respect to the hippocampus and amygdala, an effect decreased in the 5-HT_{1A} receptor knock-out mouse (Razoux et al., 2013). Inhibiting serotonin transmission with a 5-HT_{1A} antagonist leads to a broad reduction in FC within the frontal cortex, somatosensory cortex, thalamus, striatum, and DMN, consistent with the high receptor distribution in these areas (Razoux et al., 2013; Shah et al., 2016a). Given that serotonin regulates CBF and blood pressure, an agonist of the 5-$HT_{1B/1D}$ receptors that causes vasoconstriction was investigated, revealing that DMN connectivity was not affected (Shah et al., 2016a). To understand the influence of down-regulation of the serotonin transporter, which has been implicated in depression, the FC of serotonin transporter knockout rats was examined and found to be similar to that of wild-type rats despite an increased serotonin level and cocaine hyper-responsivity (van der Marel et al., 2013). This is different from human studies which showed that FC correlated with a genetic polymorphism that encodes the expression of the serotonin transporter (Wiggins et al., 2012). This difference may be due to the complete knockout rather than down-regulation in the animal model.

4.7. Potential confounds

Two major confounds need to be considered in a drug study: peripheral/vascular effects and interaction with anesthesia. A drug could induce central and peripheral effects by binding to the receptors in the periphery or via modulation of the autonomous system that regulates cardiopulmonary functions. Therefore, additional measures such as CBF, cerebral blood volume (CBV) and electrophysiology, or comparison with drugs that do not cross blood-brain barrier should be obtained for proper interpretation of the FC measures. It is also important to compare drug dosage and anesthetic level or even to use another anesthetic that acts on a different system to determine the drug-anesthesia interactions and to identify the proper challenge dose for preclinical phMRI.

5. Behavior-induced network change

Intensive learning has been found to alter FC in the resting human brain (Guerra-Carrillo et al., 2014; Lewis et al., 2009; Tambini et al., 2010). Similarly, sensory stimulation in rodents can induce enhancement of FC acutely in the somatosensory cortex as well as in regions associated with vigilance, such as the limbic and insular cortices (Li et al., 2014). Furthermore, the performance of a cued reward-seeking task can reduce the FC between nodes in the DMN-like network (Li et al., 2015a). These studies indicate that both passive and active task performance can alter RSNs.

To understand whether training can lead to long-lasting plasticity of the large-scale RSN, rats were trained in a Morris water maze for 1 or 5 days after which the RSN was assessed at 1 day and 1 week after finishing the training (Nasrallah et al., 2016a). The change in the RSN was training duration dependent, lasted several days and reorganized over time towards the cortex, which is consistent with the current theory of memory consolidation (Fig. 2A). Furthermore, the connectivity in the DMN-like network increased 1 day after the training but returned to baseline at 1 week, suggesting the early involvement of the DMN in memory consolidation (Fig. 2B). Although imaging post-learning RSNs 1 day after training using medetomidine did not affect the memory (Nasrallah et al., 2016b), one should be cautious when using this sedative immediately after learning as α2-adrenergic agonists can affect memory consolidation (Ferry and McGaugh, 2008).

Another study examined FC following exposure to an unconditioned fear stimulus from a predator's (cat) odor and found that the FC within the amygdala and medial prefrontal cortex was reduced even 1 week after the traumatic experience (Liang et al., 2014a). Together, these studies indicate the existence of persisting neural oscillations at least a week after learning and the potential of rsfMRI to track such processes in vivo. These behavior-dependent changes also suggest that variations in RSNs may arise from differences in behavioral manipulation and environmental enrichment.

6. Manipulation of networks by brain stimulation

Brain stimulation techniques, such as deep brain stimulation or transcranial current/magnetic stimulation, have become popular tools for improving motor or cognitive function or alleviating the symptoms of various disorders, although how they modulate network function is still not clear. Rodent models provide a good way to elucidate the mechanisms involved and to optimize the stimulation target and paradigm. Using deep brain stimulation, it has been shown that high frequency (130 Hz) stimulation in the external globus pallidus, substantia nigra or nucleus accumbens can transiently modulate brain-wide FC, particularly in downstream regions not directly activated by the stimulation (Albaugh et al., 2016; Van Den Berge et al., 2017). This indicates that high frequency neural oscillation could alter RSNs and the potential roles of those subcortical nuclei in shaping RSN activity. As the frequency used in deep brain stimulation is typically much higher than that seen in the RSN, how it affects the infra-slow activity of remote areas requires further

investigation. Whether very low frequency stimulation can modulate RSNs also remains to be elucidated.

In rodents, optogenetics and chemogenetics provide unique alternatives for controlling neural activity with high spatial and temporal precision. By expressing light-sensitive ion channels, such as channelrhodopsins, in neurons or astrocytes, optogenetic stimulation can be used to pinpoint the role of a particular neural pathway through cell-specific activation or inhibition (Lee et al., 2010; Zhang et al., 2007). For example, by expressing channelrhodopsins in the thalamocortical excitatory neurons in the ventral posteromedial thalamus, which projects to the somatosensory cortex, both the visually evoked activation (an area without direct projection) and the bilateral connectivity in most of the sensory cortices at the resting state could be enhanced by low frequency (1 Hz) but not high frequency (5–40 Hz) optogenetic stimulation even after the stimulation ceased (Fig. 3) (Leong et al., 2016). Similarly, low frequency stimulation of the dorsal dentate gyrus increased brain-wide interhemispheric FC and infra-slow coherence of LFP, which were reduced by injecting tetrodotoxin that suppresses excitatory activity (Chan et al., 2017). These together suggest that low frequency activity could propagate through broad cortical areas via polysynaptic pathways to modulate sensory gain and strengthen FC. They also indicate a role of the thalamus and hippocampus in regulating cortical connectivity and behavior.

Chemogenetics expresses Designer Receptors Exclusively Activated by Designer Drugs (DREADDs) in specific cell types in a similar way to optogenetics but activates/deactivates the receptors by injecting an exogenous chemical, such as clozapine-N-oxide (CNO), without the need to implant any stimulating device (Urban and Roth, 2015). As CNO has slow pharmacokinetics, the effect can last a few hours for behavioral or imaging experiments. Using this technology, Grayson et al. demonstrated that deactivating the amygdala suppressed amygdalocortical communication and corticocortical FC in monkeys (Grayson et al., 2016). In rodents, selective activation of mesolimbic or mesocortical projections from the ventral tegmental area to the nucleus accumbens or medial prefrontal cortex, respectively, has been shown to allow the observation of responses in the downstream areas despite the fact that the FC among these areas remains unchanged (Roelofs et al., 2017). Although chemogenetics cannot control the precise timing of excitation/inhibition in the same way as optogenetics, it maintains excitation/inhibition without interfering with the timing of spontaneous activity and hence may provide complementary information.

Overall, these techniques allow the manipulation of circuit activity so that the functional role of a specific pathway or cell type in behavior can be determined. Although RSNs have been associated with various behaviors and disorders, the causal relationship remains unclear. It will be useful to apply these stimulation techniques to manipulate the RSN involved in a behavior in order to validate the functional involvement of a particular network and to explore the potential of manipulation of network activity in order to improve functional performance. For example, a recent study demonstrated that silencing highly connected network hubs in a fear-conditioning task can disrupt memory consolidation, and hence confirmed the importance of network hubs in behavior (Vetere et al., 2017). Translating similar manipulation using non-invasive brain stimulation in humans may provide new avenues for the treatment of neurological and psychiatric disorders.

7. Structural connectivity affect network organization

The structural connectivity between nodes in an RSN has been inferred from fiber tracking using diffusion MRI (Greicius et al., 2009; Teipel et al., 2010). However, diffusion imaging cannot differentiate unmyelinated fibers, or the directionality, density and number of synapses crossed. Therefore, how axonal properties affect FC is still not clear. In the animal brain, anterograde (or retrograde) and monosynaptic tract tracers can be used to determine the direction and density of axonal tracts between brain regions to reveal the circuitry of the brain (Oh et al., 2014; Zingg et al., 2014). Compared with these axonal connectivity atlases, good correspondence between regions with strong direct projection and FC strength have been found in the DMN (Stafford et al., 2014) and cortical networks (Bergmann et al., 2016; Grandjean et al., 2017). As

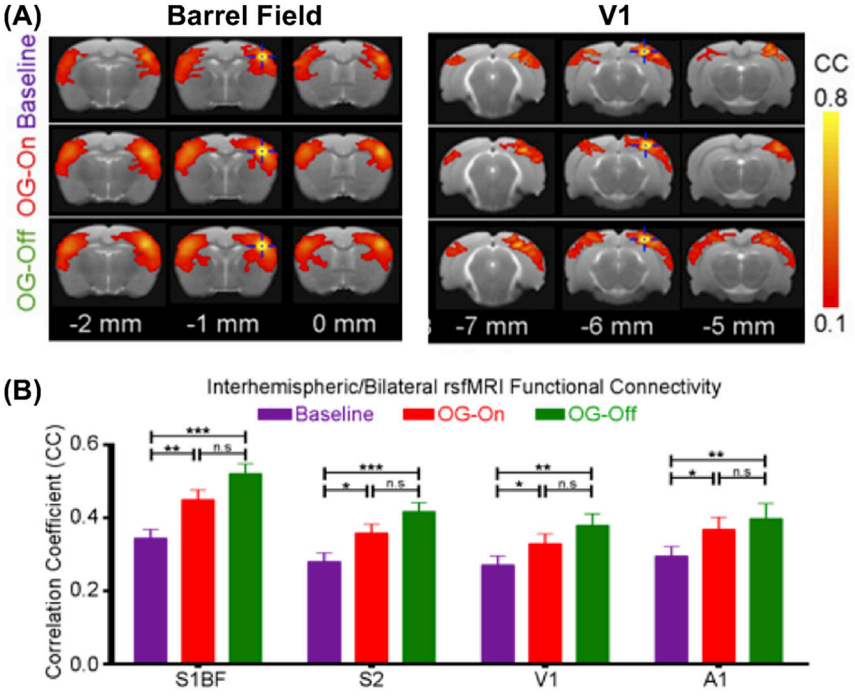

Fig. 3. Low-frequency stimulation enhances functional connectivity. (**A**) Low frequency (e.g., 1 Hz) but not high frequency (e.g., 40 Hz) optogenetic stimulation to the ventral posteromedial (VPM) thalamo-cortical excitatory neurons can enhance bilateral connectivity in cortical areas that receive a direct (e.g., barrel field) or indirect (e.g., primary visual cortex (V1)) projection. (**B**) Connectivity is enhanced during (OG-On) and after (OG-Off) the stimulation. Baseline: before stimulation; OG-On: during optogenetic (OG) stimulation; OG-Off: after stimulation. *** $P < 0.001$; ** $P < 0.01$; * $P < 0.05$; n.s., not significant. Adapted from Leong et al. (2016) with permission.

current analyses have been limited to unidirectional monosynaptic projections, further examination of bidirectional and/or polysynaptic projections between functionally connected regions will be important to elucidate the structural basis of the RSN. Using graph theory analysis, a recent study showed that cortical FC is mostly associated with monosynaptic projections whereas subcortical FC tends to depend on polysynaptic projections (Grandjean et al., 2017).

Experimental models of axonal damage, agenesis of the corpus callosum or callosotomy provide another way to understand the structural-functional interaction. Cuprizone, a toxin that damages oligodendrocytes, has been used as a model of demyelination and remyelination. With cuprizone-induced demyelination, FC strength decreases globally, with several connections in the DMN becoming negative and the correlation between white matter fractional anisotropy and FC strength disappearing (Hübner et al., 2017). Mouse models lacking a corpus callosum, such as I/LnJ or BTBR T + tpr3tf/J (BTBR) mice, allow investigation of the role of corpus callosum on the bilateral FC. Partially disrupted inter-hemispheric connectivity is found in the I/LnJ (Schroeter et al., 2017) and BTBR mice (Sforazzini et al., 2014a), indicating compensation by polysynaptic projections in the intact networks. The disrupted fronto-thalamic and striatal FC in the BTBR mice is also consistent with their autism-like behavior (Sforazzini et al., 2014a). On the other hand, complete callosotomy leads to fully disrupted bilateral FC and reduced propagation of cortical activity, which supports the role of the corpus callosum in the formation of bilateral FC (Magnuson et al., 2014b; Zhou et al., 2014). Interestingly, the bilateral connectivity gradually recovered in animals with partial callosotomy, indicating a plasticity that may be mediated by remaining projections (Zhou et al., 2014). These findings highlight the importance of axonal connectivity that subserves the RSN topology and activity, and the potential plasticity that may occur to maintain the networks and their associated functions. Further study will be needed to elucidate the specific projections or pathways that underly network topology, function and behavior.

8. Genetic and strain effects on network changes

Combining genomics and neuroimaging, recent studies have identified an association between genetic variations and brain structure and function in humans (Richiardi et al., 2015; Thompson et al., 2013). Similar exploration can be done in the mouse brain using gene expression and axonal connectivity atlases (Lein et al., 2007; Oh et al., 2014). The covariate of gene expression profiles between axonally connected regions was found to be highly coupled in regions with bidirectional connectivity and between network hubs, with genes related to the regulation of synaptic connectivity, axonogenesis and metabolism, indicating the molecular and energetic demands of maintaining neural communication (Fulcher and Fornito, 2016). The correlated expression of ion channel-related genes in the cortex also shows high similarity with the axonal connectivity in the mouse brain (Richiardi et al., 2015).

As well as revealing associations between connectivity and genes, transgenic mouse models provide a powerful tool for discovery and validation. The role of specific genes on the brain connectome can be examined using knock-in or knockout animals. For example, single gene deletion of the mu-opioid receptor gene (Oprm1) leads to extensive changes in FC, particularly in the motivational and aversion-related networks, despite minimal changes in structural connectivity (Mechling et al., 2016). The pathological effect of the TOR1A gene in early-onset generalized torsion dystonia (Dyt1), an autosomal dominant movement disorder, was evaluated in (Dyt1)ΔGAG heterozygous knock-in mice, revealing increased FC across the striatum, thalamus, and somatosensory cortex, and reduced FC in the motor and cerebellar cortices (DeSimone et al., 2016).

Genetic difference in rodent strains has also been found to affect FC. A study comparing the thalamocortical network of Brown Norway rats and Dahl salt-sensitive rats found that the former have a larger somatosensory-evoked response to electrical forepaw stimulation and more extensive but weaker FC under the resting state (Li et al., 2013). Another study compared the DMN-like connectivity in Wistar Kyoto rats and spontaneously hypertensive rats, an inbred strain originated from selected Wistar rats that have high blood pressure, and found that the former have stronger connectivity with the hippocampus whereas the hypertensive rats have stronger connectivity with the caudate putamen, which may be related to their hyperactivity (Huang et al., 2016). Using similar strains but imaging in awake condition, another study compared adolescent spontaneously hypertensive rats with two common rat strains (Wistar and Sprague Dawley) and found that the functional networks were mostly similar except for the striatal and visual networks in the hypertensive rats that may indicate their ADHD-like phenotype (Poirier et al., 2017).

In the case of mice, a study comparing C57BL/6, BALB/C and SJL mice found that the connectivity strength in both albino strains (BALB/C and SJL mice) were generally stronger than that in the C57BL/6 black mouse (Shah et al., 2016b). Part of the FC difference between strains could be due to the structural connectivity difference. In a study comparing C57BL/6 and BALB/C with a mouse model of corpus callosum agenesis, I/LnJ, bilateral FC strength did not correlate with vascular reactivity but with corpus callosum integrity measured by fractional anisotropy using diffusion tensor imaging. This was true even for the two normal mouse strains (Schroeter et al., 2017).

These studies demonstrate that rsfMRI could be a sensitive way to detect differences in genetic background and relevant behavioral phenotype. The use of genetic manipulation together with RSN mapping will be a powerful way for understanding the causal relationship between genetic variation, the functional connectome, and behavior.

9. Disease-dependent network changes

Deficits in and reorganization of RSNs have been suggested as potential biomarkers for disease progression and the evaluation of treatment. Given that the actual causes of the altered RSNs in human disorders are not clear, rsfMRI in rodent models of these diseases provides a translatable way to understand the mechanisms underlying pathologies and treatment outcomes. The recent application of such rodent models of neurological, neurodegenerative and psychiatric disorders are described below:

9.1. Brain, spinal cord and peripheral nerve injury

Human studies of traumatic brain injury (TBI) have identified various forms of dysfunction in connectivity including aberrant FC in the DMN and the salience network (Sharp et al., 2014). To date, only a few studies have applied rsfMRI in rodent models of TBI, based on either a diffuse or focal injury model. A study using the lateral fluid-percussion injury rat model, which can create injury in broad areas, identified reduced FC to the injured cortex 4 months after the injury (Mishra et al., 2014). Moreover, the animal became susceptible to epilepsy after the injury. Another study using the unilateral controlled cortical impact injury, which creates a more focal injury, found that FC is dramatically increased, rather than decreased, throughout the brain except in those areas connected to the injury site (Harris et al., 2016). The hyper-connectivity gradually reduces over 4 weeks indicating a transition from acute to chronic stage. As brain injury could damage blood vessels, or alter metabolism and other aspects of physiology depending on the severity and site of the injury, the BOLD signal could be confounded by changing neurovascular coupling during disease progression. T_2 and T_2^* may also be changed by hemorrhage and edema, particularly near the injury site, and hence affect the BOLD measurement.

One study measured FC in the somatosensory pathway following injury of the spinothalamic tract in rats (Seminowicz et al., 2012). Increased FC could be seen within the thalamus and somatosensory cortex up to 2 weeks after the spinal cord injury. In particular, there was a strong negative correlation between the thalamus and the cortex acutely

at 7 days after the injury, which coincided with the development of hypersensitivity.

Studies on peripheral nerve injury have demonstrated cortical plasticity, particularly bilateral activation when the healthy limb is stimulated (Pawela et al., 2010; Pelled et al., 2009, 2007). Nonetheless, the FC of the somatosensory system in the brain is generally reduced (Pawela et al., 2010). Interestingly, although the connectivity in the visual system is not affected, regions involved in visual-motor integration do show an effect. Another study using sciatic nerve ligation as a model for neuropathic pain reported little disruption of the RSN at 5 days after the injury but a significant effect at 28 days, particularly in the limbic system and those between the limbic and nociceptive areas (Baliki et al., 2014).

Overall, these studies indicate highly dynamic, large-scale, multisystem plasticity following an injury and the potential of rsfMRI to track this reorganization longitudinally. However, more studies are needed to determine the relationship between network plasticity, structural connectivity, and recovery from injury.

9.2. Stroke

Using transient middle cerebral artery occlusion as a model of ischemic stroke, a dramatic reduction in interhemispheric FC in the somatosensory, motor and visual cortices can be detected 1 day after stroke. The FC gradually recovers over several weeks, correlating with the recovery of sensorimotor function (van Meer et al., 2010b). Increased thalamocortical connectivity with functional recovery was also observed (Shim et al., 2017). The FC at the acute stage also negatively correlates with the infarct volume and motor function (Bauer et al., 2014). To understand the structural connectivity change, the same group further used manganese as a tract tracer injected into the contralesional motor cortex and found significantly reduced manganese transport to the ipsilesional sensorimotor cortex and increased uptake at the injection site, indicating increased local activity and reduced remote connectivity (van Meer et al., 2010a). Furthermore, the normalization of the affected bilateral connectivity back to baseline correlated with the recovery of structural connectivity in the corticospinal tract, although the structural connectivity during the acute stage had better predictive value of recovery of functional performance (van Meer et al., 2012). As stroke significantly affects vascular function and metabolism, the hemodynamic response could become slower near the infarct area, and post-processing such as global signal regression could also create artifacts in the contralateral cortex when the infarct area is large (Bauer et al., 2014).

9.3. Alzheimer's disease

Alzheimer's disease is a neurodegenerative disease that has been shown to affect RSNs, in particular the DMN and salience network, in humans. However, how the pathological process disrupts the connectivity is still not clear. Using transgenic mice that express human amyloid precursor protein (hAPP), resulting in the development of one of the major pathological hallmarks of the disease, the beta-amyloid plaques, an early study identified that the bilateral connectivity strength in young mice, measured by the optical intrinsic signal from hemoglobin, correlates with the regional amyloid plaque load in aged mice, suggesting that FC may detect regions that are vulnerable to amyloid toxicity (Bero et al., 2012). Similarly, a rsfMRI study on the same mouse model showed decreased bilateral FC (Shah et al., 2013). Reduced FC was also observed in another type of hAPP transgenic mouse even before the onset of amyloid deposition, but there was no correlation between plaque density and FC (Grandjean et al., 2014b). On the other hand, hyperconnectivity was found before the onset of amyloid deposition in two other strains of transgenic mice that express hAPP, an effect that was ameliorated by anti-amyloid antibody treatment (Shah et al., 2016c). Therefore, there appear to be mutation- and expression-dependent phenotypes. By comparing three different kinds of mice expressing amyloid plaques either intracellularly, in the parenchyma, or in both tissue and blood vessels, a recent study found that the FC change is more significant in mice which develop plaques in the parenchyma (Grandjean et al., 2016b).

Besides amyloid plaques, the influence of genetic risk factors, such as the apolipoprotein (apoE) ε4 allele, in the brain can be assessed by rsfMRI. It has been found that the FC in transgenic mice expressing human apoE ε4 is reduced in both mid-age and old mice, although perfusion deficits and reduced postsynaptic density are only seen in old mice. Therefore it is still not clear what contributes to the reduced FC in the mid-age mice (Zerbi et al., 2014). Given that apoE is involved in amyloid aggregation and clearance, it could be a drug target. One study applied anti-apoE immunotherapy to the cortical surface and found that it reduced the density of amyloid plaques and increased the bilateral FC (Liao et al., 2014). Overall, however, whether and how amyloid toxicity affects FC needs further investigation. It should be noted that a common amyloid pathology, cerebral amyloid angiopathy, which occurs concomitant with Alzheimer's disease can affect the hemodynamic response and hence confound the FC measures (Mueggler et al., 2002).

9.4. Stress and depression

Human studies of depression have found altered connectivity with the DMN, amygdala, and visual cortex (Greicius et al., 2007; Veer et al., 2010; Zeng et al., 2012). Using the Wistar Kyoto More Immobile strain which exhibits depressive-like behavior, both increased and decreased connectivity with the hippocampus was found (Williams et al., 2014). In a rat model of depression caused by prenatal stress, the FC between regions associated with the dopamine system were found to be changed, although this effect was reversed by the treatment with ladostigil, a brain-selective monoamine oxidase inhibitor (Goelman et al., 2014). A recent study which examined depression caused by chronic psychosocial stress after daily exposure to another aggressive mouse strain found increased FC within the somatosensory, visual and cingulate cortices and between the prefrontal cortex, cingulate cortex, and amygdala (Grandjean et al., 2016a). This is similar to the elevated FC in the somatosensory and visual cortices and DMN observed in a chronic stress model induced by prolonged (10 days) immobilization (Henckens et al., 2015). Another study investigated rats exposed to early life social stress induced by a novel male intruder revealing altered FC with the prefrontal cortex, nucleus accumbens, hippocampus, and somatosensory cortex (Nephew et al., 2017). Stress-related genetic effects on FC were examined in a mouse model with heterozygous knockout of a key neurodevelopmental gene, Ahi1, which leads to a stress-resilient phenotype. The amygdala connectivity of the Ahi1 knockout mice was reduced and the brain networks were highly assorted but less hierarchical (Lotan et al., 2017, 2014). To understand treatment-resistant depression, another study investigated a genetic rat model with congenital learned helplessness and found a general enhancement of FC, particularly in relation to serotonergic projections, such as those between the dorsal raphe nucleus and forebrain and in the hippocampal-prefrontal network (Gass et al., 2014a). The identification of similar networks to those in humans indicates that these models may have translational potential.

9.5. Autism spectrum disorder (ASD)

Human studies on ASD have found decreased FC in the DMN and with respect to the medial prefrontal cortex, amygdala, fusiform gyrus and insula (Nielsen et al., 2013; Sandi and Haller, 2015). Due to the multiple causes of ASD, various animal models have been explored. One study examined the Fmr1-/y mouse model of fragile X syndrome, which is a major contributor to ASD, and found reduced cortical and hippocampal connectivity (Haberl et al., 2015). Given that human subjects with corpus callosum agenesis show ASD-like symptoms, a mouse model of this deficit – the BTBR mouse – has been studied as an idiopathic model of autism, revealing reduced FC between the frontal cortex, thalamus and striatum (Sforazzini et al., 2014a). The influence

of genetic risk for ASD in the CNTNAP2 gene was assess in the CNTNAP2 knockout mouse, which showed reduced long-range FC with the cingulate cortex and hypoconnectivity between the anterior and posterior hubs of the DMN, which correlated with the observed behavioral deficit (Liska et al., 2017). To understand whether deficient neuron-microglia signaling could contribute to ASD, another study used a mouse model lacking the chemokine receptor Cx3cr1, which results in a deficit in synaptic pruning and behavior phenotype of ASD, and found broad reduction of inter-regional FC, particularly between the prefrontal cortex and hippocampus (Zhan et al., 2014). Recently, a mechanism linking immune dysfunction and behavioral impairment such as those observed in ASD has been found, with immune-deficitent SCID mice exhibiting hyperconnectivity between multiple frontal and insular regions (Filiano et al., 2016). The influence of prenatal exposure to toxins, for example domoic acid, has also been studied in the mouse revealing increased connectivity in the anterior part of the DMN but a decrease in the posterior part, as well as increased local connectivity (Mills et al., 2016). These studies demonstrate the value of connectivity imaging in rodent models in elucidating ASD associated mechanisms. As ASD is a developmental disorder, future study on the developing rodent brain are needed to further elucidate the source and progression of dys-connectivity.

9.6. Schizophrenia

Human studies on schizophrenia have found reduced strength but increased diversity of FC across the brain, particularly with respect to the prefrontal cortex and between the frontal and temporal cortices (Fornito et al., 2012; Lynall et al., 2010). Owing to the dysfunction of glutamate transmission in schizophrenia, rodent studies usually use NMDA receptor antagonists, such as PCP or ketamine, to induce schizophrenia-like phenotypes (see section 5.1 on glutamatergic effects on FC). Studies of alternative models can be summarized as follows. A study using the D-aspartate oxidase knockout mouse, which has increased D-aspartate that agonizes the NMDA receptor and shows attenuated schizophrenic behavior, found enhanced hippocampal-sensorimotor connectivity that may underscore the reduced hippocampal-temporal connectivity observed in schizophrenia patients; however, no prefrontal dys-connectivity was observed (Errico et al., 2015). In a rat model of schizophrenia that involved prenatal exposure to a toxin, methylazoxymethanol acetate, a broad reduction in orbitofrontal connectivity but an increase in visual connectivity was found, in line with the altered metabolism and glutamate-glutamine cycling in these areas (Kaneko et al., 2017). Recently, the genetic effect of 15q13.3 microdeletion copy number variation in schizophrenia was studied in a mouse model (Gass et al., 2016). The FC was found to be generally increased in this mouse. As part of the gene encodes nicotinic acetylcholine alpha 7 receptors, the FC could be restored to normal by positively modulating the receptor.

10. Physiological considerations during experiments

A major challenge of rsfMRI is the rejection of signal variations of non-neural origin, such as system instability, motion and physiological artifacts (see (Keilholz et al., 2016; Liu, 2016) for review). Physiological variations could affect hemodynamic-based FC measures in two ways: temporal modulation of the BOLD signal, or a change of baseline neural activity and BOLD signal due to an altered basal physiological state. The baseline physiology difference could come from between-group differences in cardiopulmonary and vascular functions due to aging, disease or various interventions. Although many methods have been proposed to account for these, some of them, particularly the baseline difference, can not be easily removed. Given that physiology can be controlled more tightly in animals than in humans, these confounds could potentially be minimized. The major physiological factors are discussed below.

10.1. Respiratory and cardiac artifacts

Cardiac pulsation and respiration are the most well-recognized sources of physiological variation in the BOLD signal. They affect the BOLD signal via physiological changes in partial pressure of O_2 (pO_2) and CO_2 (pCO_2), CBF, intracranial pressure and cerebrospinal fluid (CSF) flow, but also through physical modulation of the magnetic field due to the susceptibility change caused by chest motion. Resting-state BOLD signal has been found to covariate with respiratory cycle/depth and cardiac cycle (Chuang and Chen, 2001), the slow fluctuation in the heart rate (Shmueli et al., 2007), and breathing volume (Birn et al., 2006; Chang and Glover, 2009).

In the rodent brain, cardiac artifacts tend to localize near large blood vessels, the sagittal sinus and brain base, whereas respiratory artifacts are more widespread and stronger, with affected regions extending further around ventricles (Kalthoff et al., 2011; Majeed et al., 2009). The respiration-induced magnetic field variation can lead to image shifting along the phase encoding direction of the echo-planar imaging (EPI) at ultrahigh magnetic field (Kalthoff et al., 2011). As the heart rate (200–600 beats per minute) and respiration rate (50–120 breaths per minute) in anesthetized rodents are much faster than the typical imaging rate (repetition time $\geq$ 1s), these artifacts can be aliased to anywhere within the Nyquist frequency, and hence cannot be removed simply by low-pass filtering.

These confounds can be reduced by post-processing either based on the recorded cardiac pulsation and respiration (Glover et al., 2000), or by estimating such nuisance signal regressors from the fMRI data using ICA (Griffanti et al., 2014) or from the white matter and CSF using principal component analysis (Behzadi et al., 2007). However, if the respiratory or heart rate differs between groups, these corrections may not be able to account for systemic differences. However, using intubation with mechanical ventilation to minimize variation in the respiratory rate and volume can mitigate part of the difference.

10.2. Variation in body temperature

Fluctuations in the body temperature of anesthetized animals can alter the BOLD signal globally even when the temperature change is within the physiological range (Vanhoutte et al., 2006). It has been shown that the BOLD signal negatively correlates with body temperature, whereby a temperature increase of 2 °C can lead to ~6% BOLD signal decrease at 7 T (Vanhoutte et al., 2006). The BOLD signal change is partly due to the temperature-dependent change is the apparent transverse relaxation time (T_2*) and partly due to changes in spontaneous neural activity (Reig et al., 2010). Consequently, its effect can not be easily corrected. It is therefore important to maintain a constant body temperature during any fMRI study.

10.3. Baseline difference in blood CO_2 and O_2

Arterial blood CO_2 and O_2 levels reflect the balance between metabolic demand, ventilation and vascular regulation. They have profound effects on both the evoked and resting-state BOLD signals via their vasodilatory and vasoconstrictive effects, respectively, together with changes in vascular reactivity and blood oxygenation. The influence of temporal variation in blood CO_2 on FC has been associated with respiratory artifacts. Given that the ventilation and vascular responses could vary depending on the experimental setup, disease or intervention, the resultant baseline difference in blood CO_2 and O_2 could lead to another confound. In humans, the resting end-tidal CO_2 level is associated with a difference in vascular reactivity which in turn changes FC strength (Golestani et al., 2016). By maintaining animals under mild hypercapnia, increased CBF and a slower and smaller BOLD response can be observed, whereas decreased CBF and a faster and larger BOLD response can be seen under hypocapnia (Cohen et al., 2002; Kemna and Posse, 2001). Such hemodynamic differences may lead to changes in the amplitude and

frequency of the resting-state BOLD signal. By altering the steady-state pCO_2 and pO_2 in the blood, we have shown that hyperoxia can increase the overall connectivity strength and fluctuation amplitude, whereas changing pCO_2 alone and keeping pO_2 constant has a marginal effect, suggesting that pO_2 has stronger effect on the BOLD signal (Nasrallah et al., 2015). Furthermore, the oscillating frequency distribution changes with increasing blood CO_2 level, correlating with increased coherence of LFP, particularly in the gamma band. These results indicate that neural synchrony, not just the hemodynamic response, could change under systemic physiological baseline changes. Therefore, it is important to maintain normal pO_2 and pCO_2 by careful ventilation control and monitoring. Keeping animals under 100% O_2, which leads to hyperoxia, is not a desirable condition for fMRI.

10.4. Baseline difference in blood pressure

Blood pressure is a major vascular factor that can alter both the resting and evoked BOLD signals. Cerebrovascular autoregulation maintains constant CBF despite a change in arterial blood pressure. In anesthetized rodents, the CBF does not change with blood pressure variations within 40–130 mmHg (Dalkara et al., 1995; Gozzi et al., 2007). However, as a drug challenge could cause the blood pressure to exceed that range, the CBF could change proportionally and induce a distributed BOLD signal change (Gozzi et al., 2007; Luo et al., 2003). Milder blood pressure changes (e.g., within 10 mmHg) induced by sensory stimulation could also elicit a BOLD signal change (Wang et al., 2006), and a change induced by pain stimulation could even alter the neurovascular coupling (Uchida et al., 2017), which would complicate the evoked and resting fMRI measures under such pathological conditions. More importantly, fluctuations in blood pressure and heart rate have been reported to explain nearly half of the variance in the spontaneous hemodynamic fluctuation even with normal blood pressure (Katura et al., 2006). Therefore, blood pressure variations could confound resting BOLD connectivity measures, similar to cardiac artifacts.

In addition to the temporal variation, the basal level of blood pressure could modulate the BOLD signal oscillation. Based on exsanguination and reinfusion of blood in rats, the drop in blood pressure has been shown to increase the low-frequency BOLD signal amplitudes and inter-regional correlation throughout the brain, with the largest increase being observed in the cortex (Biswal and Kannurpatti, 2009). The concomitant blood pressure change induced by a drug could also confound the BOLD response to the drug. For example, when a peripheral vasoconstrictor, phenylephrine, was used to control blood pressure, the BOLD signal change induced by a dopamine receptor agonist, apomorphine, became positive rather than negative (Kalisch et al., 2005). Although the effect of chronic blood pressure changes in disease models with spontaneous hypertension or altered vascular function, such as stroke, is not clear, controlling blood pressure should be considered important to rule out this physiological confound.

10.5. Baseline differences in CBF or CBV

The baseline CBF or CBV serves as an indicator of vascular function and metabolic activity. The BOLD activation amplitude has been found to correlate with baseline CBF or CBV, suggesting that vascular differences could be responsible for individual BOLD signal variations in human subjects (Liau and Liu, 2009) and in mice (Schroeter et al., 2017). The regional CBF has been shown to correlate with FC strength and long-range connectivity in humans, which may be related to higher metabolic demand in functional hubs that integrating long-range information (Liang et al., 2013a). As there could be a larger baseline CBF/CBV difference due to age, disease stage and intervention (such as exercise or diet), this physiological information should be recorded to improve the interpretation of observed FC differences.

11. Technical considerations in data processing

Most rodent rsfMRI studies follow similar procedures to those designed for humans. However, due to the very different brain size, shape and tissue proportions, there are several aspects related to post-processing and analysis that need to be considered.

11.1. Susceptibility artifacts

The magnetic field distortion at the air-tissue interface is generally far more severe in rodents than in humans due to the much smaller size of the brain and higher field strength used in rodent imaging. This leads to geometric distortion and signal void in EPI, particularly in the olfactory bulb and cerebellum (due to poorer shimming away from the center), around the perirhinal cortex and amygdala (due to the ear canal) and on top of the neocortex (due to the proximity to air). Such effects severely hinder the measurement of whole-brain FC and the localization accuracy. As the geometric distortion leads to dispersion/compression of spins to/from different locations, the intensity distortion cannot be corrected by nonlinear registration even if this could undistort the shape (Hong et al., 2015). Susceptibility artifacts can be reduced by applying susceptibility matching materials, such as gel, on top of the brain (Adamczak et al., 2010) or injecting fomblin into the inner ear (Li et al., 2015b). Spin-echo acquisition could be used but with a trade-off on BOLD sensitivity (Harris et al., 2015; Nasrallah et al., 2012b). Post-processing using a reversed-phase EPI data can effectively reduce geometric and intensity distortion but not signal void (Hong et al., 2015). Its efficacy for gradient-echo EPI is also inferior to that of spin-echo. Multi-echo EPI could compensate part of the signal void by acquiring data at short echo time (Kundu et al., 2014). Combining multi-echo acquisition and reversed phase correction would improve the mapping of the whole brain.

11.2. Motion artifacts

Motion correction is typically applied to rsfMRI data. As most rodent imaging is conducted under anesthesia with the head secured, the head motion is expected to be minimal. The motion correction algorithm is more likely to reflect the signal variation from other sources, such as a respiration-induced shift in the phase encoding direction (Kalthoff et al., 2011). Therefore, unless there is movement in the image, correcting pseudo-motion may introduce an artifact into the signal.

11.3. Physiological artifacts

Although various methods for correcting respiratory and cardiac artifacts in rsfMRI have been proposed, some approaches may not be optimal for rodents. For example, the CSF and white matter in the rodent brain are much smaller and were difficult to segment from low-resolution rsfMRI data without the partial volume with the gray matter. The muscle around the head, which is not seen in humans, may be used to capture the relatively global respiratory artifacts. As physiological artifacts could lead to fluctuations with both positive and negative correlation (Kalthoff et al., 2011), independent or principal component-based methods would be more suitable than using the averaged signal as a nuisance regressor (Behzadi et al., 2007). Another source of physiological artifacts could be movement of the jaw and tongue, which can result in intensity variations or even geometric distortion. These can be minimized by the use of padding to reduce jaw movement.

11.4. Global signal regression

Global signal regression/normalization has been used in several rsfMRI studies in humans to reduce global variation and improve

localization. As the majority of the rodent brain is gray matter as opposed to the human brain where the majority is white matter, this processing can remove certain large-scale neural activity, such as the burst-suppression activity (Liu et al., 2011). Furthermore, it can lead to increased negative correlation in rodents (Kalthoff et al., 2013), similar to what has been shown in humans (Murphy et al., 2009), or even the removal of connectivity entirely (Bergmann et al., 2016). Recently, a globally propagating wave of neuronal Ca^{2+} activity has been found to underlie the global hemodynamic wave and the co-activation of the RSN (Matsui et al., 2016), indicating an important role of global neural activity. Therefore, the use of global signal regression should be carefully evaluated and validated.

11.5. Filter bandwidth

Due to the slow hemodynamic response, most rsfMRI studies only use signal fluctuations <0.1 Hz to measure FC. As highlighted in the section on anesthesia effects, certain anesthetics may shift the activity to a higher frequency. In addition, oscillations at even higher frequency (>0.5 Hz) have been shown to present similar network organization and may provide additional information on the dynamics of RSNs (Chan et al., 2015; Lee et al., 2013). Therefore, a wider bandwidth would be needed to avoid removing critical information.

11.6. Seed-based analysis vs ICA

The connectivity detected by ICA is typically confined within a functional area (e.g., somatosensory cortex or hippocampus; see Fig. 1B) either bilaterally, unilaterally or along the anteroposterior axis (e.g., cingulate cortex), rather than cross-functional areas (Jonckers et al., 2011; Liang et al., 2011; Mechling et al., 2014; Zerbi et al., 2015). Therefore it may not be sensitive enough to detect highly distributed networks such as the DMN (Sforazzini et al., 2014b) without considerable data averaging (Lu et al., 2012). On the other hand, seed-based analysis, besides being more sensitive in detecting the DMN, could also reveal more detailed connectivity among associated areas in a system or pathway, such as the lateral genicular nucleus, superior colliculus and visual cortex within the visual pathway (Pawela et al., 2008). It could also differentiate sub-regional connectivity, such as thalamocortical connections of each area in the thalamus (Liang et al., 2013b), sub-regional connections in the striatum (Grandjean et al., 2017) or even layer-specific FC patterns (Baek et al., 2016). Therefore, the method of choice will depend on the hypothesis being tested.

12. Conclusion

RSNs in the rodent brain not only show similar topology to those of human, but their changes in response to manipulations and in disease models indicate tremendous translational potential. With the same technique, rsfMRI, that can be applied to both humans and animal models, observations in humans can be validated in animal models and new hypotheses/interventions can be evaluated/optimized in animal models before applying them to humans. The application of invasive tools, such as neurophysiology, axonal tracing and histopathology, and comparison of disease models of various pathogenic mechanisms will help to elucidate the neural and pathological bases of the RSNs observed in human. The availability of genetic tools in rodents, such as optogenetics, chemogenetics and transgenic animals, further allows the identification of the effects of a specific protein, receptor, cell type, or neuronal pathway on the RSN. This will allow researchers to tease out the role of a particular neuronal oscillation, brain region, pathway or network on the behavior or disorder. However, considering the variability that occurs due to methodology, efforts should be made to standardize the anesthesia protocol, physiological control, data processing, quality control and brain template to facilitate the comparison and combination of data across laboratories. For example, measuring sensory evoked activation would be a good way to evaluate the physiological condition and data quality, but such data is usually not acquired. An alternative is to assess the consistency in detecting the stereotypical connectivity patterns described in the section 2.1. Similar approach has been used in human studies to evaluate denoising methods for rsfMRI (Pruim et al., 2015). As this result could provide information not only on the data quality but also the baseline condition of the experiment, it should be reported in addition to network changes under manipulation.

Acknowledgement

We would like to thank the funding support of the Motor Accident and Insurance Commission, Australia (Nasrallah) and the Queensland Brain Institute (Chuang). We thank Ms Rowan Tweedale for proof reading, and Dr Valerio Zerbi for providing data for the figure.

References

Adamczak, J.M., Farr, T.D., Seehafer, J.U., Kalthoff, D., Hoehn, M., 2010. High field BOLD response to forepaw stimulation in the mouse. Neuroimage 51, 704–712. https://doi.org/10.1016/j.neuroimage.2010.02.083.

Albaugh, D.L., Salzwedel, A., Van Den Berge, N., Gao, W., Stuber, G.D., Shih, Y.-Y.I., 2016. Functional magnetic resonance imaging of electrical and optogenetic deep brain stimulation at the rat nucleus accumbens. Sci. Rep. 6, 31613. https://doi.org/10.1038/srep31613.

Ash, J.A., Lu, H., Taxier, L.R., Long, J.M., Yang, Y., Stein, E.A., Rapp, P.R., 2016. Functional connectivity with the retrosplenial cortex predicts cognitive aging in rats. Proc. Natl. Acad. Sci. U. S. A. 113, 12286–12291. https://doi.org/10.1073/pnas.1525309113.

Avsaroglu, H., van der Sar, A.S., van Lith, H.A., van Zutphen, L.F.M., Hellebrekers, L.J., 2007. Differences in response to anaesthetics and analgesics between inbred rat strains. Lab. Anim. 41, 337–344. https://doi.org/10.1258/002367707781282811.

Baek, K., Shim, W.H., Jeong, J., Radhakrishnan, H., Rosen, B.R., Boas, D., Franceschini, M., Biswal, B.B., Kim, Y.R., 2016. Layer-specific interhemispheric functional connectivity in the somatosensory cortex of rats: resting state electrophysiology and fMRI studies. Brain Struct. Funct. 221, 2801–2815. https://doi.org/10.1007/s00429-015-1073-0.

Baliki, M.N., Chang, P.C., Baria, A.T., Centeno, M.V., Apkarian, A.V., 2014. Resting-sate functional reorganization of the rat limbic system following neuropathic injury. Sci. Rep. 4, 6186. https://doi.org/10.1038/srep06186.

Barttfeld, P., Uhrig, L., Sitt, J.D., Sigman, M., Jarraya, B., Dehaene, S., 2015. Signature of consciousness in the dynamics of resting-state brain activity. Proc. Natl. Acad. Sci. 112, 887–892. https://doi.org/10.1073/pnas.1418031112.

Bauer, A.Q., Kraft, A.W., Wright, P.W., Snyder, A.Z., Lee, J.M., Culver, J.P., 2014. Optical imaging of disrupted functional connectivity following ischemic stroke in mice. Neuroimage 99, 388–401. https://doi.org/10.1016/j.neuroimage.2014.05.051.

Becerra, L., Pendse, G., Chang, P.-C., Bishop, J., Borsook, D., 2011. Robust reproducible resting state networks in the awake rodent brain. PLoS One 6, e25701. https://doi.org/10.1371/journal.pone.0025701.

Behzadi, Y., Restom, K., Liau, J., Liu, T.T., 2007. A component based noise correction method (CompCor) for BOLD and perfusion based fMRI. Neuroimage 37, 90–101. https://doi.org/10.1016/j.neuroimage.2007.04.042.

Bennett, B.D., Huguenard, J.R., Prince, D.A., 1998. Adrenergic modulation of GABAA receptor-mediated inhibition in rat sensorimotor cortex. J. Neurophysiol. 79, 937–946.

Berger, M., Gray, J.A., Roth, B.L., 2009. The expanded biology of serotonin. Annu. Rev. Med. 60, 355–366. https://doi.org/10.1146/annurev.med.60.042307.110802.

Bergmann, E., Zur, G., Bershadsky, G., Kahn, I., 2016. The organization of mouse and human cortico-hippocampal networks estimated by intrinsic functional connectivity. Cereb. Cortex 26, 4497–4512. https://doi.org/10.1093/cercor/bhw327.

Bergonzi, K.M., Bauer, A.Q., Wright, P.W., Culver, J.P., 2015. Mapping functional connectivity using cerebral blood flow in the mouse brain. J. Cereb. Blood Flow. Metab. 35, 367–370. https://doi.org/10.1038/jcbfm.2014.211.

Bero, A.W., Bauer, A.Q., Stewart, F.R., White, B.R., Cirrito, J.R., Raichle, M.E., Culver, J.P., Holtzman, D.M., 2012. Bidirectional relationship between functional connectivity and amyloid-β deposition in mouse brain. J. Neurosci. 32, 4334–4340. https://doi.org/10.1523/JNEUROSCI.5845-11.2012.

Bettinardi, R.G., Tort-Colet, N., Ruiz-Mejias, M., Sanchez-Vives, M.V., Deco, G., 2015. Gradual emergence of spontaneous correlated brain activity during fading of general anesthesia in rats: evidences from fMRI and local field potentials. Neuroimage 114, 185–198. https://doi.org/10.1016/j.neuroimage.2015.03.037.

Birn, R.M., Diamond, J.B., Smith, M.A., Bandettini, P.A., 2006. Separating respiratory-variation-related fluctuations from neuronal-activity-related fluctuations in fMRI. Neuroimage 31, 1536–1548. https://doi.org/10.1016/j.neuroimage.2006.02.048.

Biswal, B.B., Kannurpatti, S.S., 2009. Resting-state functional connectivity in animal models: modulations by exsanguination. Methods Mol. Biol., Methods Mol. Biol. 489, 255–274. https://doi.org/10.1007/978-1-59745-543-5.

Brynildsen, J.K., Hsu, L.-M., Ross, T.J., Stein, E.A., Yang, Y., Lu, H., 2017. Physiological characterization of a robust survival rodent fMRI method. Magn. Reson. Imaging 35, 54–60. https://doi.org/10.1016/j.mri.2016.08.010.

Bukhari, Q., Schroeter, A., Cole, D.M., Rudin, M., 2017. Resting state fMRI in mice reveals anesthesia specific signatures of brain functional networks and their interactions. Front. Neural Circuits 11. https://doi.org/10.3389/fncir.2017.00005.

Calhoun, V.D., Sui, J., Kiehl, K., Turner, J., Allen, E., Pearlson, G., 2012. Exploring the psychosis functional connectome: aberrant intrinsic networks in schizophrenia and bipolar disorder. Front. Psychiatry 2, 1–13. https://doi.org/10.3389/fpsyt.2011.00075.

Cauli, B., Tong, X.-K., Rancillac, A., Serluca, N., Lambolez, B., Rossier, J., Hamel, E., 2004. Cortical GABA interneurons in neurovascular coupling: relays for subcortical vasoactive pathways. J. Neurosci. 24, 8940–8949. https://doi.org/10.1523/JNEUROSCI.3065-04.2004.

Chan, A.W., Mohajerani, M.H., LeDue, J.M., Wang, Y.T., Murphy, T.H., 2015. Mesoscale infraslow spontaneous membrane potential fluctuations recapitulate high-frequency activity cortical motifs. Nat. Commun. 6, 7738. https://doi.org/10.1038/ncomms8738.

Chan, R.W., Leong, A.T.L., Ho, L.C., Gao, P.P., Wong, E.C., Dong, C.M., Wang, X., He, J., Chan, Y.-S., Lim, L.W., Wu, E.X., 2017. Low-frequency hippocampal–cortical activity drives brain-wide resting-state functional MRI connectivity. Proc. Natl. Acad. Sci. https://doi.org/10.1073/pnas.1703309114, 201703309.

Chang, C., Glover, G.H., 2009. Relationship between respiration, end-tidal CO2, and BOLD signals in resting-state fMRI. Neuroimage 47, 1381–1393. https://doi.org/10.1016/j.neuroimage.2009.04.048.

Chang, P.-C., Procissi, D., Bao, Q., Centeno, M.V., Baria, A., Apkarian, A.V., 2016. Novel method for functional brain imaging in awake minimally restrained rats. J. Neurophysiol. 116, 61–80. https://doi.org/10.1152/jn.01078.2015.

Chemali, J.J., Kenny, J.D., Olutola, O., Taylor, N.E., Kimchi, E.Y., Purdon, P.L., Brown, E.N., Solt, K., 2015. Ageing delays emergence from general anaesthesia in rats by increasing anaesthetic sensitivity in the brain. Br. J. Anaesth. 115 (Suppl. l), i58–i65. https://doi.org/10.1093/bja/aev112.

Chuang, K.H., Chen, J.H., 2001. IMPACT: image-based physiological artifacts estimation and correction technique for functional MRI. Magn. Reson. Med. 46, 344–353. https://doi.org/10.1002/mrm.1197.

Cinnamon Bidwell, L., Dew, R.E., Kollins, S.H., 2010. Alpha-2 adrenergic receptors and attention-deficit/hyperactivity disorder. Curr. Psychiatry Rep. 12, 366–373. https://doi.org/10.1007/s11920-010-0136-4.

Cohen, E.R., Ugurbil, K., Kim, S., 2002. Effect of basal conditions on the magnitude and dynamics of the blood oxygenation level-dependent fMRI response. J. Cereb. Blood Flow. Metab. 22, 1042–1053. https://doi.org/10.1097/00004647-200209000-00002.

Colon-Perez, L.M., Tran, K., Thompson, K., Pace, M.C., Blum, K., Goldberger, B.A., Gold, M.S., Bruijnzeel, A.W., Setlow, B., Febo, M., 2016. The psychoactive designer drug and bath salt constituent MDPV causes widespread disruption of brain functional connectivity. Neuropsychopharmacology 41, 2352–2365. https://doi.org/10.1038/npp.2016.40.

Colonnese, M.T., Phillips, M.A., Constantine-Paton, M., Kaila, K., Jasanoff, A., 2008. Development of hemodynamic responses and functional connectivity in rat somatosensory cortex. Nat. Neurosci. 11, 72–79. https://doi.org/10.1038/nn2017.

Dalkara, T., Irikura, K., Huang, Z., Panahian, N., Moskowitz, M.A., 1995. Cerebrovascular responses under controlled and monitored physiological conditions in the anesthetized mouse. J. Cereb. Blood Flow. Metab. 15, 631–638. https://doi.org/10.1038/jcbfm.1995.79.

DeSimone, J.C., Febo, M., Shukla, P., Ofori, E., Colon-Perez, L.M., Li, Y., Vaillancourt, D.E., 2016. In vivo imaging reveals impaired connectivity across cortical and subcortical networks in a mouse model of DYT1 dystonia. Neurobiol. Dis. 95, 35–45. https://doi.org/10.1016/j.nbd.2016.07.005.

Ellenbroek, B., Youn, J., 2016. Rodent models in neuroscience research: is it a rat race? Dis. Model. Mech. 9, 1079–1087. https://doi.org/10.1242/dmm.026120.

Errico, F., D'Argenio, V., Sforazzini, F., Iasevoli, F., Squillace, M., Guerri, G., Napolitano, F., Angrisano, T., Di Maio, A., Keller, S., Vitucci, D., Galbusera, A., Chiariotti, L., Bertolino, A., de Bartolomeis, A., Salvatore, F., Gozzi, A., Usiello, A., 2015. A role for D-aspartate oxidase in schizophrenia and in schizophrenia-related symptoms induced by phencyclidine in mice. Transl. Psychiatry 5, e512. https://doi.org/10.1038/tp.2015.2.

Fergus, A., Lee, K.S., 1997. GABAergic regulation of cerebral microvascular tone in the rat. J. Cereb. Blood Flow. Metab. 17, 992–1003. https://doi.org/10.1097/00004647-199709000-00009.

Ferry, B., McGaugh, J.L., 2008. Involvement of basolateral amygdala alpha2-adrenoceptors in modulating consolidation of inhibitory avoidance memory. Learn. Mem. 15, 238–243. https://doi.org/10.1101/lm.760908.

Filiano, A.J., Xu, Y., Tustison, N.J., Marsh, R.L., Baker, W., Smirnov, I., Overall, C.C., Gadani, S.P., Turner, S.D., Weng, Z., Peerzade, S.N., Chen, H., Lee, K.S., Scott, M.M., Beenhakker, M.P., Litvak, V., Kipnis, J., 2016. Unexpected role of interferon-γ in regulating neuronal connectivity and social behaviour. Nature 535, 425–429. https://doi.org/10.1038/nature18626.

Fornito, A., Zalesky, A., Pantelis, C., Bullmore, E.T., 2012. Schizophrenia, neuroimaging and connectomics. Neuroimage 62, 2296–2314. https://doi.org/10.1016/j.neuroimage.2011.12.090.

Fox, M.D., Snyder, A.Z., Vincent, J.L., Corbetta, M., Van Essen, D.C., Raichle, M.E., 2005. The human brain is intrinsically organized into dynamic, anticorrelated functional networks. Proc. Natl. Acad. Sci. U. S. A. 102, 9673–9678. https://doi.org/10.1073/pnas.0504136102.

Fukuda, M., Vazquez, A.L., Zong, X., Kim, S.-G., 2013. Effects of the α_2-adrenergic receptor agonist dexmedetomidine on neural, vascular and BOLD fMRI responses in the somatosensory cortex. Eur. J. Neurosci. 37, 80–95. https://doi.org/10.1111/ejn.12024.

Fulcher, B.D., Fornito, A., 2016. A transcriptional signature of hub connectivity in the mouse connectome. Proc. Natl. Acad. Sci. U. S. A. 113 https://doi.org/10.1073/pnas.1513302113, 1513302113-.

Gao, Y.-R., Ma, Y., Zhang, Q., Winder, A.T., Liang, Z., Antinori, L., Drew, P.J., Zhang, N., 2016. Time to wake up: studying neurovascular coupling and brain-wide circuit function in the un-anesthetized animal. Neuroimage 0–1. https://doi.org/10.1016/j.neuroimage.2016.11.069.

Gass, N., Cleppien, D., Zheng, L., Schwarz, A.J., Meyer-Lindenberg, A., Vollmayr, B., Weber-Fahr, W., Sartorius, A., 2014a. Functionally altered neurocircuits in a rat model of treatment-resistant depression show prominent role of the habenula. Eur. Neuropsychopharmacol. 24, 381–390. https://doi.org/10.1016/j.euroneuro.2013.12.004.

Gass, N., Schwarz, A.J., Sartorius, A., Cleppien, D., Zheng, L., Schenker, E., Risterucci, C., Meyer-Lindenberg, A., Weber-Fahr, W., 2013. Haloperidol modulates midbrain-prefrontal functional connectivity in the rat brain. Eur. Neuropsychopharmacol. 23, 1310–1319. https://doi.org/10.1016/j.euroneuro.2012.10.013.

Gass, N., Schwarz, A.J., Sartorius, A., Schenker, E., Risterucci, C., Spedding, M., Zheng, L., Meyer-Lindenberg, A., Weber-Fahr, W., 2014b. Sub-anesthetic ketamine modulates intrinsic BOLD connectivity within the hippocampal-prefrontal circuit in the rat. Neuropsychopharmacology 39, 895–906. https://doi.org/10.1038/npp.2013.290.

Gass, N., Weber-Fahr, W., Sartorius, A., Becker, R., Didriksen, M., Stensbøl, T.B., Bastlund, J.F., Meyer-Lindenberg, A., Schwarz, A.J., 2016. An acetylcholine alpha7 positive allosteric modulator rescues a schizophrenia-associated brain endophenotype in the 15q13.3 microdeletion, encompassing CHRNA7. Eur. Neuropsychopharmacol. 26, 1150–1160. https://doi.org/10.1016/j.euroneuro.2016.03.013.

Glover, G.H., Li, T.Q., Ress, D., 2000. Image-based method for retrospective correction of physiological motion effects in fMRI: RETROICOR. Magn. Reson. Med. 44, 162–167.

Goelman, G., Ilinca, R., Zohar, I., Weinstock, M., 2014. Functional connectivity in prenatally stressed rats with and without maternal treatment with ladostigil, a brain-selective monoamine oxidase inhibitor. Eur. J. Neurosci. 40, 2734–2743. https://doi.org/10.1111/ejn.12621.

Golestani, A.M., Kwinta, J.B., Strother, S.C., Khatamian, Y.B., Chen, J.J., 2016. The association between cerebrovascular reactivity and resting-state fMRI functional connectivity in healthy adults: the influence of basal carbon dioxide. Neuroimage 132, 301–313. https://doi.org/10.1016/j.neuroimage.2016.02.051.

Gozzi, A., Ceolin, L., Schwarz, A., Reese, T., Bertani, S., Crestan, V., Bifone, A., 2007. A multimodality investigation of cerebral hemodynamics and autoregulation in pharmacological MRI. Magn. Reson. Imaging 25, 826–833. https://doi.org/10.1016/j.mri.2007.03.003.

Gozzi, A., Schwarz, A., Crestan, V., Bifone, A., 2008. Drug-anaesthetic interaction in phMRI: the case of the psychotomimetic agent phencyclidine. Magn. Reson. Imaging 26, 999–1006. https://doi.org/10.1016/j.mri.2008.01.012.

Grandjean, J., Azzinnari, D., Seuwen, A., Sigrist, H., Seifritz, E., Pryce, C.R., Rudin, M., 2016a. Chronic psychosocial stress in mice leads to changes in brain functional connectivity and metabolite levels comparable to human depression. Neuroimage 142, 544–552. https://doi.org/10.1016/j.neuroimage.2016.08.013.

Grandjean, J., Derungs, R., Kulic, L., Welt, T., Henkelman, M., Nitsch, R.M., Rudin, M., 2016b. Complex interplay between brain function and structure during cerebral amyloidosis in APP transgenic mouse strains revealed by multi-parametric MRI comparison. Neuroimage 134, 1–11. https://doi.org/10.1016/j.neuroimage.2016.03.042.

Grandjean, J., Schroeter, A., Batata, I., Rudin, M., 2014a. Optimization of anesthesia protocol for resting-state fMRI in mice based on differential effects of anesthetics on functional connectivity patterns. Neuroimage 102P2, 838–847. https://doi.org/10.1016/j.neuroimage.2014.08.043.

Grandjean, J., Schroeter, A., He, P., Tanadini, M., Keist, R., Krstic, D., Konietzko, U., Klohs, J., Nitsch, R.M., Rudin, M., 2014b. Early alterations in functional connectivity and white matter structure in a transgenic mouse model of cerebral amyloidosis. J. Neurosci. 34, 13780–13789. https://doi.org/10.1523/JNEUROSCI.4762-13.2014.

Grandjean, J., Zerbi, V., Balsters, J., Wenderoth, N., Rudina, M., 2017. The structural basis of large-scale functional connectivity in the mouse. J. Neurosci. 37, 8092–8101.

Grayson, D.S., Bliss-Moreau, E., Machado, C.J., Bennett, J., Shen, K., Grant, K.A., Fair, D.A., Amaral, D.G., 2016. The rhesus monkey connectome predicts disrupted functional networks resulting from pharmacogenetic inactivation of the amygdala. Neuron 91, 453–466. https://doi.org/10.1016/j.neuron.2016.06.005.

Greicius, M.D., Flores, B.H., Menon, V., Glover, G.H., Solvason, H.B., Kenna, H., Reiss, A.L., Schatzberg, A.F., 2007. Resting-state functional connectivity in major depression: abnormally increased contributions from subgenual cingulate cortex and thalamus. Biol. Psychiatry 62, 429–437. https://doi.org/10.1016/j.biopsych.2006.09.020.

Greicius, M.D., Supekar, K., Menon, V., Dougherty, R.F., 2009. Resting-state functional connectivity reflects structural connectivity in the default mode network. Cereb. Cortex 19, 72–78. https://doi.org/10.1093/cercor/bhn059.

Griffanti, L., Salimi-Khorshidi, G., Beckmann, C.F., Auerbach, E.J., Douaud, G., Sexton, C.E., Zsoldos, E.E.E., Ebmeier, K.P., Filippini, N., Mackay, C.E., Moeller, S., Xu, J., Yacoub, E., Baselli, G., Ugurbil, K., Miller, K.L., Smith, S.M., 2014. ICA-based artefact removal and accelerated fMRI acquisition for improved resting state network imaging. Neuroimage 95, 232–247. https://doi.org/10.1016/j.neuroimage.2014.03.034.

Gsell, W., Burke, M., Wiedermann, D., Bonvento, G., Silva, A.C., Dauphin, F., Bühle, C., Hoehn, M., Schwindt, W., 2006. Differential effects of NMDA and AMPA glutamate receptors on functional magnetic resonance imaging signals and evoked neuronal activity during forepaw stimulation of the rat. J. Neurosci. 26, 8409–8416. https://doi.org/10.1523/JNEUROSCI.4615-05.2006.

Guerra-Carrillo, B., Mackey, A.P., Bunge, S.A., 2014. Resting-state fMRI: a window into human brain plasticity. Neuroscientist. https://doi.org/10.1177/1073858414524442.

Haberl, M.G., Zerbi, V., Veltien, A., Ginger, M., Heerschap, A., Frick, A., 2015. Structural-functional connectivity deficits of neocortical circuits in the Fmr1 (-/y) mouse model of autism. Sci. Adv. 1, e1500775. https://doi.org/10.1126/sciadv.1500775.

Hara, K., Harris, R.A., 2002. The anesthetic mechanism of urethane: the effects on neurotransmitter-gated ion channels. Anesth. Analg. 94, 313–318. https://doi.org/10.1213/00000539-200202000-00015 table of contents.

Harris, A.P., Lennen, R.J., Marshall, I., Jansen, M.A., Pernet, C.R., Brydges, N.M., Duguid, I.C., Holmes, M.C., 2015. Imaging learned fear circuitry in awake mice using fMRI. Eur. J. Neurosci. 42, 2125–2134. https://doi.org/10.1111/ejn.12939.

Harris, N.G., Verley, D.R., Gutman, B.A., Thompson, P.M., Yeh, H.J., Brown, J.A., 2016. Disconnection and hyper-connectivity underlie reorganization after TBI: a rodent functional connectomic analysis. Exp. Neurol. 277, 124–138. https://doi.org/10.1016/j.expneurol.2015.12.020.

Henckens, M.J.A.G., Marel, K. Van Der, Toorn, A. Van Der, Pillai, A.G., Fernández, G., Dijkhuizen, R.M., Joëls, M., 2015. Stress-induced alterations in large-scale functional networks of the rodent brain. Neuroimage 105, 312–322. https://doi.org/10.1016/j.neuroimage.2014.10.037.

Hodkinson, D.J., de Groote, C., McKie, S., Deakin, J.F.W., Williams, S.R., 2012. Differential effects of anaesthesia on the phMRI response to acute ketamine challenge. Br. J. Med. Med. Res. 2, 373–385.

Hong, X., To, X.V., Teh, I., Soh, J.R., Chuang, K.-H., 2015. Evaluation of EPI distortion correction methods for quantitative MRI of the brain at high magnetic field. Magn. Reson. Imaging 33, 1098–1105. https://doi.org/10.1016/j.mri.2015.06.010.

Hsu, L., Liang, X., Gu, H., Brynildsen, J.K., Stark, J.A., Ash, J.A., Lin, C., Lu, H., Rapp, P.R., Stein, E.A., Yang, Y., 2016. Constituents and functional implications of the rat default mode network. Proc. Natl. Acad. Sci. 113, E4541–E4547. https://doi.org/10.1073/pnas.1601485113.

Hu, Y., Chen, X., Gu, H., Yang, Y., 2013. Resting-state glutamate and GABA concentrations predict task-induced deactivation in the default mode network. J. Neurosci. 33, 18566–18573. https://doi.org/10.1523/JNEUROSCI.1973-13.2013.

Huang, S.-M., Wu, Y.-L., Peng, S.-L., Peng, H.-H., Huang, T.-Y., Ho, K.-C., Wang, F.-N., 2016. Inter-strain differences in default mode network: a resting state fMRI study on spontaneously hypertensive rat and wistar Kyoto rat. Sci. Rep. 6, 21697. https://doi.org/10.1038/srep21697.

Hübner, N.S., Mechling, A.E., Lee, H., Reisert, M., Bienert, T., Hennig, J., von Elverfeldt, D., Harsan, L.-A., 2017. The connectomics of brain demyelination: functional and structural patterns in the cuprizone mouse model. Neuroimage 146, 1–18. https://doi.org/10.1016/j.neuroimage.2016.11.008.

Hudetz, A.G., 2012. General anesthesia and human brain connectivity. Brain Connect. 2, 291–302. https://doi.org/10.1089/brain.2012.0107.

Hutchison, R.M., Hutchison, M., Manning, K.Y., Menon, R.S., Everling, S., 2014. Isoflurane induces dose-dependent alterations in the cortical connectivity profiles and dynamic properties of the brain's functional architecture. Hum. Brain Mapp. 35, 5754–5775. https://doi.org/10.1002/hbm.22583.

Hutchison, R.M., Mirsattari, S.M., Jones, C.K., Gati, J.S., Leung, L.S., 2010. Functional networks in the anesthetized rat brain revealed by independent component analysis of resting-state FMRI. J. Neurophysiol. 103, 3398–3406. https://doi.org/10.1152/jn.00141.2010.

Janssen, B.J.A., De Celle, T., Debets, J.J.M., Brouns, A.E., Callahan, M.F., Smith, T.L., 2004. Effects of anesthetics on systemic hemodynamics in mice. Am. J. Physiol. Heart Circ. Physiol. 287, H1618–H1624. https://doi.org/10.1152/ajpheart.01192.2003.

Jonckers, E., Delgado y Palacios, R., Shah, D., Guglielmetti, C., Verhoye, M., Van der Linden, A., 2014. Different anesthesia regimes modulate the functional connectivity outcome in mice. Magn. Reson. Med. 72, 1103–1112. https://doi.org/10.1002/mrm.24990.

Jonckers, E., Shah, D., Hamaide, J., Verhoye, M., Van der Linden, A., 2015. The power of using functional fMRI on small rodents to study brain pharmacology and disease. Front. Pharmacol. 6, 1–19. https://doi.org/10.3389/fphar.2015.00231.

Jonckers, E., Van Audekerke, J., De Visscher, G., Van der Linden, A., Verhoye, M., 2011. Functional connectivity fMRI of the rodent brain: comparison of functional connectivity networks in rat and mouse. PLoS One 6, e18876. https://doi.org/10.1371/journal.pone.0018876.

Kalisch, R., Delfino, M., Murer, M.G., Auer, D.P., 2005. The phenylephrine blood pressure clamp in pharmacologic magnetic resonance imaging: reduction of systemic confounds and improved detectability of drug-induced BOLD signal changes. Psychopharmacol. Berl. 180, 774–780. https://doi.org/10.1007/s00213-005-2252-0.

Kalthoff, D., Po, C., Wiedermann, D., Hoehn, M., 2013. Reliability and spatial specificity of rat brain sensorimotor functional connectivity networks are superior under sedation compared with general anesthesia. NMR Biomed. 26, 638–650. https://doi.org/10.1002/nbm.2908.

Kalthoff, D., Seehafer, J.U., Po, C., Wiedermann, D., Hoehn, M., 2011. Functional connectivity in the rat at 11.7T: impact of physiological noise in resting state fMRI. Neuroimage 54, 2828–2839. https://doi.org/10.1016/j.neuroimage.2010.10.053.

Kaneko, G., Sanganahalli, B.G., Groman, S.M., Wang, H., Coman, D., Rao, J., Herman, P., Jiang, L., Rich, K., de Graaf, R.A., Taylor, J.R., Hyder, F., 2017. Hypofrontality and posterior hyperactivity in early schizophrenia: imaging and behavior in a preclinical model. Biol. Psychiatry 81, 503–513. https://doi.org/10.1016/j.biopsych.2016.05.019.

Kapur, S., Seeman, P., 2002. NMDA receptor antagonists ketamine and PCP have direct effects on the dopamine D(2) and serotonin 5-HT(2)receptors-implications for models of schizophrenia. Mol. Psychiatry 7, 837–844. https://doi.org/10.1038/sj.mp.4001093.

Katura, T., Tanaka, N., Obata, A., Sato, H., Maki, A., 2006. Quantitative evaluation of interrelations between spontaneous low-frequency oscillations in cerebral hemodynamics and systemic cardiovascular dynamics. Neuroimage 31, 1592–1600. https://doi.org/10.1016/j.neuroimage.2006.02.010.

Keilholz, S.D., Pan, W.-J., Billings, J., Nezafati, M., Shakil, S., 2016. Noise and non-neuronal contributions to the BOLD signal: applications to and insights from animal studies. Neuroimage. https://doi.org/10.1016/j.neuroimage.2016.12.019.

Kemna, L.J., Posse, S., 2001. Effect of respiratory CO(2) changes on the temporal dynamics of the hemodynamic response in functional MR imaging. Neuroimage 14, 642–649. https://doi.org/10.1006/nimg.2001.0859.

Kocsis, P., Gyertyán, I., Eles, J., Laszy, J., Hegedűs, N., Gajári, D., Deli, L., Pozsgay, Z., Dávid, S., Tihanyi, K., 2014. Vascular action as the primary mechanism of cognitive effects of cholinergic, CNS-acting drugs, a rat phMRI BOLD study. J. Cereb. Blood Flow. Metab. 34, 995–1000. https://doi.org/10.1038/jcbfm.2014.47.

Kundu, P., Santin, M.D., Bandettini, P.A., Bullmore, E.T., Petiet, A., 2014. Differentiating BOLD and non-BOLD signals in fMRI time series from anesthetized rats using multi-echo EPI at 11.7T. Neuroimage 102, 861–874. https://doi.org/10.1016/j.neuroimage.2014.07.025.

Lee, H.-L., Zahneisen, B., Hugger, T., LeVan, P., Hennig, J., 2013. Tracking dynamic resting-state networks at higher frequencies using MR-encephalography. Neuroimage 65, 216–222. https://doi.org/10.1016/j.neuroimage.2012.10.015.

Lee, J.H., Durand, R., Gradinaru, V., Zhang, F., Goshen, I., Kim, D.-S., Fenno, L.E., Ramakrishnan, C., Deisseroth, K., 2010. Global and local fMRI signals driven by neurons defined optogenetically by type and wiring. Nature 465, 788–792. https://doi.org/10.1038/nature09108.

Lein, E.S., Hawrylycz, M.J., Ao, N., Ayres, M., Bensinger, A., Bernard, A., Boe, A.F., Boguski, M.S., Brockway, K.S., Byrnes, E.J., Chen, L., Chen, L., Chen, T.-M., Chin, M.C., Chong, J., Crook, B.E., Czaplinska, A., Dang, C.N., Datta, S., Dee, N.R., Desaki, A.L., Desta, T., Diep, E., Dolbeare, T.A., Donelan, M.J., Dong, H.-W., Dougherty, J.G., Duncan, B.J., Ebbert, A.J., Eichele, G., Estin, L.K., Faber, C., Facer, B.A., Fields, R., Fischer, S.R., Fliss, T.P., Frensley, C., Gates, S.N., Glattfelder, K.J., Halverson, K.R., Hart, M.R., Hohmann, J.G., Howell, M.P., Jeung, D.P., Johnson, R.A., Karr, P.T., Kawal, R., Kidney, J.M., Knapik, R.H., Kuan, C.L., Lake, J.H., Laramee, A.R., Larsen, K.D., Lau, C., Lemon, T.A., Liang, A.J., Liu, Y., Luong, L.T., Michaels, J., Morgan, J.J., Morgan, R.J., Mortrud, M.T., Mosqueda, N.F., Ng, L.L., Ng, R., Orta, G.J., Overly, C.C., Pak, T.H., Parry, S.E., Pathak, S.D., Pearson, O.C., Puchalski, R.B., Riley, Z.L., Rockett, H.R., Rowland, S.A., Royall, J.J., Ruiz, M.J., Sarno, N.R., Schaffnit, K., Shapovalova, N.V., Sivisay, T., Slaughterbeck, C.R., Smith, S.C., Smith, K.A., Smith, B.I., Sodt, A.J., Stewart, N.N., Stumpf, K.-R., Sunkin, S.M., Sutram, M., Tam, A., Teemer, C.D., Thaller, C., Thompson, C.L., Varnam, L.R., Visel, A., Whitlock, R.M., Wohnoutka, P.E., Wolkey, C.K., Wong, V.Y., Wood, M., Yaylaoglu, M.B., Young, R.C., Youngstrom, B.L., Yuan, X.F., Zhang, B., Zwingman, T.A., Jones, A.R., 2007. Genome-wide atlas of gene expression in the adult mouse brain. Nature 445, 168–176. https://doi.org/10.1038/nature05453.

Leong, A.T.L., Chan, R.W., Gao, P.P., Chan, Y.-S., Tsia, K.K., Yung, W.-H., Wu, E.X., 2016. Long-range projections coordinate distributed brain-wide neural activity with a specific spatiotemporal profile. Proc. Natl. Acad. Sci. U. S. A. 113, E8306–E8315. https://doi.org/10.1073/pnas.1616361113.

Lewis, C.M., Baldassarre, A., Committeri, G., Romani, G.L., Corbetta, M., 2009. Learning sculpts the spontaneous activity of the resting human brain. Proc. Natl. Acad. Sci. U. S. A. 106, 17558–17563. https://doi.org/10.1073/pnas.0902455106.

Li, C., Li, Z., Ward, D., Dwinell, M.R., Lombard, J.H., Hudetz, A.G., Pawela, C.P., 2014a. Enhancement of resting-state fcMRI networks by prior sensory stimulation. Brain Connect. 4, 1–26. https://doi.org/10.1089/brain.2014.0326.

Li, J., Ishiwari, K., Conway, M.W., Francois, J., Huxter, J., Lowry, J.P., Schwarz, A.J., Tricklebank, M., Gilmour, G., 2014b. Dissociable effects of antipsychotics on ketamine-induced changes in regional oxygenation and inter-regional coherence of low frequency oxygen fluctuations in the rat. Neuropsychopharmacology 39, 1635–1644. https://doi.org/10.1038/npp.2014.10.

Li, J., Martin, S., Tricklebank, M.D., Schwarz, X.A.J., Gilmour, G., 2015a. Task-induced modulation of intrinsic functional connectivity networks in the behaving rat. J. Neurosci. 35, 658–665. https://doi.org/10.1523/JNEUROSCI.3488-14.2015.

Li, R., Liu, X., Sidabras, J.W., Paulson, E.S., Jesmanowicz, A., Nencka, A.S., Hudetz, A.G., Hyde, J.S., 2015b. Restoring susceptibility induced MRI signal loss in rat brain at 9.4 T: a step towards whole brain functional connectivity imaging. PLoS One 10, e0119450. https://doi.org/10.1371/journal.pone.0119450.

Li, W., Antuono, P.G., Xie, C., Chen, G., Jones, J.L., Ward, B.D., Franczak, M.B., Goveas, J.S., Li, S.-J., 2012. Changes in regional cerebral blood flow and functional connectivity in the cholinergic pathway associated with cognitive performance in subjects with mild Alzheimer's disease after 12-week donepezil treatment. Neuroimage 60, 1083–1091. https://doi.org/10.1016/j.neuroimage.2011.12.077.

Li, Z., Ward, B.D., Dwinell, M.R., Lombard, J.H., Pawela, C.P., 2013. FMRI and fcMRI phenotypes map the genomic effect of chromosome 13 in Brown Norway and Dahl salt-sensitive rats. Neuroimage 90, 403–412. https://doi.org/10.1016/j.neuroimage.2013.09.049.

Liang, X., Zou, Q., He, Y., Yang, Y., 2013a. Coupling of functional connectivity and regional cerebral blood flow reveals a physiological basis for network hubs of the human brain. Proc. Natl. Acad. Sci. 110, 1929–1934. https://doi.org/10.1073/pnas.1214900110.

Liang, Z., King, J., Zhang, N., 2014a. Neuroplasticity to a single-episode traumatic stress revealed by resting-state fMRI in awake rats. Neuroimage 103, 485–491. https://doi.org/10.1016/j.neuroimage.2014.08.050.

Liang, Z., King, J., Zhang, N., 2012a. Anticorrelated resting-state functional connectivity in awake rat brain. Neuroimage 59, 1190–1199. https://doi.org/10.1016/j.neuroimage.2011.08.009.

Liang, Z., King, J., Zhang, N., 2012b. Intrinsic organization of the anesthetized brain. J. Neurosci. 32, 10183–10191. https://doi.org/10.1523/JNEUROSCI.1020-12.2012.
Liang, Z., King, J., Zhang, N., 2011. Uncovering intrinsic connectional architecture of functional networks in awake rat brain. J. Neurosci. 31, 3776–3783. https://doi.org/10.1523/JNEUROSCI.4557-10.2011.
Liang, Z., Li, T., King, J., Zhang, N., 2013b. Mapping thalamocortical networks in rat brain using resting-state functional connectivity. Neuroimage 83, 237–244. https://doi.org/10.1016/j.neuroimage.2013.06.029.
Liang, Z., Liu, X., Zhang, N., 2014b. Dynamic resting state functional connectivity in awake and anesthetized rodents. Neuroimage 104, 89–99. https://doi.org/10.1016/j.neuroimage.2014.10.013.
Liao, F., Hori, Y., Hudry, E., Bauer, A.Q., Jiang, H., Mahan, T.E., Lefton, K.B., Zhang, T.J., Dearborn, J.T., Kim, J., Culver, J.P., Betensky, R., Wozniak, D.F., Hyman, B.T., Holtzman, D.M., 2014. Anti-ApoE antibody given after plaque onset decreases aβ accumulation and improves brain function in a mouse model of aβ amyloidosis. J. Neurosci. 34, 7281–7292. https://doi.org/10.1523/JNEUROSCI.0646-14.2014.
Liau, J., Liu, T.T., 2009. Inter-subject variability in hypercapnic normalization of the BOLD fMRI response. Neuroimage 45, 420–430. https://doi.org/10.1016/j.neuroimage.2008.11.032.
Liska, A., Bertero, A., Gomolka, R., Sabbioni, M., Galbusera, A., Barsotti, N., Panzeri, S., Scattoni, M.L., Pasqualetti, M., Gozzi, A., 2017. Homozygous loss of autism-risk gene CNTNAP2 results in reduced local and long-range prefrontal functional connectivity. Cereb. Cortex 1–13. https://doi.org/10.1093/cercor/bhx022 (in press).
Liska, A., Galbusera, A., Schwarz, A.J., Gozzi, A., 2015. Functional connectivity hubs of the mouse brain. Neuroimage 115, 281–291. https://doi.org/10.1016/j.neuroimage.2015.04.033.
Liu, T.T., 2016. Noise contributions to the fMRI signal: an overview. Neuroimage 143, 141–151. https://doi.org/10.1016/j.neuroimage.2016.09.008.
Liu, X., Pillay, S., Li, R., Vizuete, J.A., Pechman, K.R., Schmainda, K.M., Hudetz, A.G., 2013a. Multiphasic modification of intrinsic functional connectivity of the rat brain during increasing levels of propofol. Neuroimage 83, 581–592. https://doi.org/10.1016/j.neuroimage.2013.07.003.
Liu, X., Zhu, X.-H., Zhang, Y., Chen, W., 2013b. The change of functional connectivity specificity in rats under various anesthesia levels and its neural origin. Brain Topogr. 26, 363–377. https://doi.org/10.1007/s10548-012-0267-5.
Liu, X., Zhu, X.H., Zhang, Y., Chen, W., 2011. Neural origin of spontaneous hemodynamic fluctuations in rats under burst-suppression anesthesia condition. Cereb. Cortex 21, 374–384. https://doi.org/10.1093/cercor/bhq105.
Liu, J.V., Hirano, Y., Nascimento, G.C., Stefanovic, B., Leopold, D.A., Silva, A.C., 2013c. fMRI in the awake marmoset: somatosensory-evoked responses, functional connectivity, and comparison with propofol anesthesia. Neuroimage 78, 186–195. https://doi.org/10.1016/j.neuroimage.2013.03.038.
Lotan, A., Lifschytz, T., Mernick, B., Lory, O., Levi, E., Ben-Shimol, E., Goelman, G., Lerer, B., 2017. Alterations in the expression of a neurodevelopmental gene exert long-lasting effects on cognitive-emotional phenotypes and functional brain networks: translational evidence from the stress-resilient Ahi1 knockout mouse. Mol. Psychiatry 22, 884–899. https://doi.org/10.1038/mp.2016.29.
Lotan, a, Lifschytz, T., Slonimsky, A., Broner, E.C., Greenbaum, L., Abedat, S., Fellig, Y., Cohen, H., Lory, O., Goelman, G., Lerer, B., 2014. Neural mechanisms underlying stress resilience in Ahi1 knockout mice: relevance to neuropsychiatric disorders. Mol. Psychiatry 19, 243–252. https://doi.org/10.1038/mp.2013.123.
Low, L.A., Bauer, L.C., Klaunberg, B.A., 2016a. Comparing the effects of isoflurane and alpha chloralose upon mouse physiology. PLoS One 11, e0154936. https://doi.org/10.1371/journal.pone.0154936.
Low, L.A., Bauer, L.C., Pitcher, M.H., Bushnell, M.C., 2016b. Restraint training for awake functional brain scanning of rodents can cause long-lasting changes in pain and stress responses. Pain 157, 1. https://doi.org/10.1097/j.pain.0000000000000579.
Lu, H., Zou, Q., Gu, H., Raichle, M.E., Stein, E.A., Yang, Y., 2012. Rat brains also have a default mode network. Proc. Natl. Acad. Sci. U. S. A. 109, 3979–3984. https://doi.org/10.1073/pnas.1200506109.
Lu, H., Zuo, Y., Gu, H., Waltz, J.A., Zhan, W., Scholl, C.A., Rea, W., Yang, Y., Stein, E.A., 2007. Synchronized delta oscillations correlate with the resting-state functional MRI signal. Proc. Natl. Acad. Sci. U. S. A. 104, 18265–18269. https://doi.org/10.1073/pnas.0705791104.
Luo, F., Wu, G., Li, Z., Li, S.-J., 2003. Characterization of effects of mean arterial blood pressure induced by cocaine and cocaine methiodide on BOLD signals in rat brain. Magn. Reson. Med. 49, 264–270. https://doi.org/10.1002/mrm.10366.
Lynall, M., Bassett, D.S., Kerwin, R., McKenna, P.J., Kitzbichler, M., Muller, U., Bullmore, E., 2010. Functional connectivity and brain networks in schizophrenia. J. Neurosci. 30, 9477–9487. https://doi.org/10.1523/JNEUROSCI.0333-10.2010.
Ma, Y., Shaik, M.A., Kozberg, M.G., Kim, S.H., Portes, J.P., Timerman, D., Hillman, E.M.C., 2016a. Resting-state hemodynamics are spatiotemporally coupled to synchronized and symmetric neural activity in excitatory neurons. Proc. Natl. Acad. Sci. U. S. A. 113, E8463–E8471. https://doi.org/10.1073/pnas.1525369113.
Ma, Z., Perez, P., Ma, Z., Liu, Y., Hamilton, C., Liang, Z., Zhang, N., 2016b. Functional atlas of the awake rat brain: a neuroimaging study of rat brain specialization and integration. Neuroimage. https://doi.org/10.1016/j.neuroimage.2016.07.007.
Magnuson, M.E., Thompson, G.J., Pan, W.-J., Keilholz, S.D., 2014a. Time-dependent effects of isoflurane and dexmedetomidine on functional connectivity, spectral characteristics, and spatial distribution of spontaneous BOLD fluctuations. NMR Biomed. 27, 291–303. https://doi.org/10.1002/nbm.3062.
Magnuson, M.E., Thompson, G.J., Pan, W.-J., Keilholz, S.D., 2014b. Effects of severing the corpus callosum on electrical and BOLD functional connectivity and spontaneous dynamic activity in the rat brain. Brain Connect. 4, 15–29. https://doi.org/10.1089/brain.2013.0167.
Majeed, W., Magnuson, M., Keilholz, S.D., 2009. Spatiotemporal dynamics of low frequency fluctuations in BOLD fMRI of the rat. J. Magn. Reson. Imaging 30, 384–393. https://doi.org/10.1002/jmri.21848.
Masamoto, K., Fukuda, M., Vazquez, A., Kim, S.-G., 2009. Dose-dependent effect of isoflurane on neurovascular coupling in rat cerebral cortex. Eur. J. Neurosci. 30, 242–250. https://doi.org/10.1111/j.1460-9568.2009.06812.x.
Masamoto, K., Kanno, I., 2012. Anesthesia and the quantitative evaluation of neurovascular coupling. J. Cereb. Blood Flow. Metab. 32, 1233–1247. https://doi.org/10.1038/jcbfm.2012.50.
Matsui, T., Murakami, T., Ohki, K., 2016. Transient neuronal coactivations embedded in globally propagating waves underlie resting-state functional connectivity. Proc. Natl. Acad. Sci. 113, 201521299. https://doi.org/10.1073/pnas.1521299113.
Mechling, A., Hübner, N., Lee, H.-L., Hennig, J., von Elverfeldt, D., Harsan, L.-A., 2014. Fine-grained mapping of mouse brain functional connectivity with resting-state fMRI. Neuroimage 96C, 203–215. https://doi.org/10.1016/j.neuroimage.2014.03.078.
Mechling, A.E., Arefin, T., Lee, H.-L., Bienert, T., Reisert, M., Ben Hamida, S., Darcq, E., Ehrlich, A., Gaveriaux-Ruff, C., Parent, M.J., Rosa-Neto, P., Hennig, J., von Elverfeldt, D., Kieffer, B.L., Harsan, L.-A., 2016. Deletion of the mu opioid receptor gene in mice reshapes the reward-aversion connectome. Proc. Natl. Acad. Sci. U. S. A. 113, 11603–11608. https://doi.org/10.1073/pnas.1601640113.
Medda, A., Hoffmann, L., Magnuson, M., Thompson, G., Pan, W.J., Keilholz, S., 2016. Wavelet-based clustering of resting state MRI data in the rat. Magn. Reson. Imaging 34, 35–43. https://doi.org/10.1016/j.mri.2015.10.005.
Mills, B.D., Pearce, H.L., Khan, O., Jarrett, B.R., Fair, D.A., Lahvis, G.P., 2016. Prenatal domoic acid exposure disrupts mouse pro-social behavior and functional connectivity MRI. Behav. Brain Res. 308, 14–23. https://doi.org/10.1016/j.bbr.2016.03.039.
Mishra, A.M., Bai, X., Sanganahalli, B.G., Waxman, S.G., Shatillo, O., Grohn, O., Hyder, F., Pitkänen, A., Blumenfeld, H., 2014. Decreased resting functional connectivity after traumatic brain injury in the rat. PLoS One 9, e95280. https://doi.org/10.1371/journal.pone.0095280.
Mueggler, T., Sturchler-Pierrat, C., Baumann, D., Rausch, M., Staufenbiel, M., Rudin, M., 2002. Compromised hemodynamic response in amyloid precursor protein transgenic mice. J. Neurosci. 22, 7218–7224 doi:20026680.
Murphy, K., Birn, R.M., Handwerker, D.A., Jones, T.B., Bandettini, P.A., 2009. The impact of global signal regression on resting state correlations: are anti-correlated networks introduced? Neuroimage 44, 893–905. https://doi.org/10.1016/j.neuroimage.2008.09.036.
Muthukumaraswamy, S.D., Edden, R.A.E., Jones, D.K., Swettenham, J.B., Singh, K.D., 2009. Resting GABA concentration predicts peak gamma frequency and fMRI amplitude in response to visual stimulation in humans. Proc. Natl. Acad. Sci. U. S. A. 106, 8356–8361. https://doi.org/10.1073/pnas.0900728106.
Nallasamy, N., Tsao, D.Y., 2011. Functional connectivity in the brain: effects of anesthesia. Neuroscientist 17, 94–106. https://doi.org/10.1177/1073858410374126.
Nasrallah, F.A., Lee, E.L.Q., Chuang, K.-H., 2012a. Optimization of flow-sensitive alternating inversion recovery (FAIR) for perfusion functional MRI of rodent brain. NMR Biomed. 25, 1209–1216. https://doi.org/10.1002/nbm.2790.
Nasrallah, F.A., Lew, S.K., Low, A.S.-M., Chuang, K.-H., 2014a. Neural correlate of resting-state functional connectivity under α2 adrenergic receptor agonist, medetomidine. Neuroimage 84, 27–34. https://doi.org/10.1016/j.neuroimage.2013.08.004.
Nasrallah, F.A., Low, S.-M.A., Lew, S.K., Chen, K., Chuang, K.-H., 2014b. Pharmacological insight into neurotransmission origins of resting-state functional connectivity: α2-adrenergic agonist vs antagonist. Neuroimage 103, 364–373. https://doi.org/10.1016/j.neuroimage.2014.09.004.
Nasrallah, F.A., Singh, K.K.D.R., Yeow, L.Y., Chuang, K.-H., 2017. GABAergic effect on resting-state functional connectivity: dynamics under pharmacological antagonism. Neuroimage 149, 53–62. https://doi.org/10.1016/j.neuroimage.2017.01.040.
Nasrallah, F.A., Tan, J., Chuang, K.-H., 2012b. Pharmacological modulation of functional connectivity: α2-adrenergic receptor agonist alters synchrony but not neural activation. Neuroimage 60, 436–446. https://doi.org/10.1016/j.neuroimage.2011.12.026.
Nasrallah, F.A., Tay, H., Chuang, K.-H., 2014c. Detection of functional connectivity in the resting mouse brain. Neuroimage 86, 417–424. https://doi.org/10.1016/j.neuroimage.2013.10.025.
Nasrallah, F.A., To, X.V., Chen, D.-Y., Routtenberg, A., Chuang, K.-H., 2016a. Functional connectivity MRI tracks memory networks after maze learning in rodents. Neuroimage 127, 196–202. https://doi.org/10.1016/j.neuroimage.2015.08.013.
Nasrallah, F.A., To, X.V., Chen, D.-Y., Routtenberg, A., Chuang, K.-H., 2016b. Resting state functional connectivity data supports detection of cognition in the rodent brain. Data Br. 7, 1156–1164. https://doi.org/10.1016/j.dib.2016.03.041.
Nasrallah, F.A., Yeow, L.Y., Biswal, B., Chuang, K.-H., 2015. Dependence of BOLD signal fluctuation on arterial blood CO2 and O2: implication for resting-state functional connectivity. Neuroimage 117, 29–39. https://doi.org/10.1016/j.neuroimage.2015.05.035.
Nephew, B.C., Huang, W., Poirier, G.L., Payne, L., King, J.A., 2017. Altered neural connectivity in adult female rats exposed to early life social stress. Behav. Brain Res. 316, 225–233. https://doi.org/10.1016/j.bbr.2016.08.051.
Nielsen, J.A., Zielinski, B.A., Fletcher, P.T., Alexander, A.L., Lange, N., Bigler, E.D., Lainhart, J.E., Anderson, J.S., 2013. Multisite functional connectivity MRI classification of autism: ABIDE results. Front. Hum. Neurosci. 7, 599. https://doi.org/10.3389/fnhum.2013.00599.
Northoff, G., Walter, M., Schulte, R.F., Beck, J., Dydak, U., Henning, A., Boeker, H., Grimm, S., Boesiger, P., 2007. GABA concentrations in the human anterior cingulate cortex predict negative BOLD responses in fMRI. Nat. Neurosci. 10, 1515–1517. https://doi.org/10.1038/nn2001.

Oh, S.W., Harris, J.A., Ng, L., Winslow, B., Cain, N., Mihalas, S., Wang, Q., Lau, C., Kuan, L., Henry, A.M., Mortrud, M.T., Ouellette, B., Nguyen, T.N., Sorensen, S.A., Slaughterbeck, C.R., Wakeman, W., Li, Y., Feng, D., Ho, A., Nicholas, E., Hirokawa, K.E., Bohn, P., Joines, K.M., Peng, H., Hawrylycz, M.J., Phillips, J.W., Hohmann, J.G., Wohnoutka, P., Gerfen, C.R., Koch, C., Bernard, A., Dang, C., Jones, A.R., Zeng, H., 2014. A mesoscale connectome of the mouse brain. Nature 508, 207–214. https://doi.org/10.1038/nature13186.

Osmanski, B.-F., Pezet, S., Ricobaraza, A., Lenkei, Z., Tanter, M., 2014. Functional ultrasound imaging of intrinsic connectivity in the living rat brain with high spatiotemporal resolution. Nat. Commun. 5, 5023. https://doi.org/10.1038/ncomms6023.

Paasonen, J., Salo, R.A., Huttunen, J.K., Gröhn, O., 2016. Resting-state functional MRI as a tool for evaluating brain hemodynamic responsiveness to external stimuli in rats. Magn. Reson. Med. 0, 21–24. https://doi.org/10.1002/mrm.26496.

Paasonen, J., Salo, R.A., Ihalainen, J., Leikas, J.V., Savolainen, K., Lehtonen, M., Forsberg, M.M., Gröhn, O., 2017. Dose-response effect of acute phencyclidine on functional connectivity and dopamine levels, and their association with schizophrenia-like symptom classes in rat. Neuropharmacology 119, 15–25. https://doi.org/10.1016/j.neuropharm.2017.03.024.

Pan, W.-J., Thompson, G.J., Magnuson, M.E., Jaeger, D., Keilholz, S., 2013. Infraslow LFP correlates to resting-state fMRI BOLD signals. Neuroimage 74, 288–297. https://doi.org/10.1016/j.neuroimage.2013.02.035.

Pan, W.J., Billings, J.C.W., Grooms, J.K., Shakil, S., Keilholz, S.D., 2015. Considerations for resting state functional MRI and functional connectivity studies in rodents. Front. Neurosci. 9, 269. https://doi.org/10.3389/fnins.2015.00269.

Pawela, C.P., Biswal, B.B., Cho, Y.R., Kao, D.S., Li, R., Jones, S.R., Schulte, M.L., Matloub, H.S., Hudetz, A.G., Hyde, J.S., 2008. Resting-state functional connectivity of the rat brain. Magn. Reson. Med. 59, 1021–1029. https://doi.org/10.1002/mrm.21524.

Pawela, C.P., Biswal, B.B., Hudetz, A.G., Li, R., Jones, S.R., Cho, Y.R., Matloub, H.S., Hyde, J.S., 2010. Interhemispheric neuroplasticity following limb deafferentation detected by resting-state functional connectivity magnetic resonance imaging (fcMRI) and functional magnetic resonance imaging (fMRI). Neuroimage 49, 2467–2478. https://doi.org/10.1016/j.neuroimage.2009.09.054.

Pawela, C.P., Biswal, B.B., Hudetz, A.G., Schulte, M.L., Li, R., Jones, S.R., Cho, Y.R., Matloub, H.S., Hyde, J.S., 2009. A protocol for use of medetomidine anesthesia in rats for extended studies using task-induced BOLD contrast and resting-state functional connectivity. Neuroimage 46, 1137–1147. https://doi.org/10.1016/j.neuroimage.2009.03.004.

Pelled, G., Bergstrom, D.A., Tierney, P.L., Conroy, R.S., Chuang, K.-H., Yu, D., Leopold, D.A., Walters, J.R., Koretsky, A.P., 2009. Ipsilateral cortical fMRI responses after peripheral nerve damage in rats reflect increased interneuron activity. Proc. Natl. Acad. Sci. U. S. A. 106, 14114–14119.

Pelled, G., Chuang, K.-H., Dodd, S.J., Koretsky, A.P., 2007. Functional MRI detection of bilateral cortical reorganization in the rodent brain following peripheral nerve deafferentation. Neuroimage 37, 262–273.

Petrinovic, M.M., Hankov, G., Schroeter, A., Bruns, A., Rudin, M., von Kienlin, M., Künnecke, B., Mueggler, T., 2016. A novel anesthesia regime enables neurofunctional studies and imaging genetics across mouse strains. Sci. Rep. 6, 24523. https://doi.org/10.1038/srep24523.

Picciotto, M.R., Higley, M.J., Mineur, Y.S., 2012. Acetylcholine as a neuromodulator: cholinergic signaling shapes nervous system function and behavior. Neuron 76, 116–129. https://doi.org/10.1016/j.neuron.2012.08.036.

Poirier, G.L., Huang, W., Tam, K., DiFranza, J.R., King, J.A., 2017. Awake whole-brain functional connectivity alterations in the adolescent spontaneously hypertensive rat feature visual streams and striatal networks. Brain Struct. Funct. 222, 1673–1683. https://doi.org/10.1007/s00429-016-1301-2.

Pruim, R.H.R., Mennes, M., Buitelaar, J.K., Beckmann, C.F., 2015. Evaluation of ICA-AROMA and alternative strategies for motion artifact removal in resting state fMRI. Neuroimage 112, 278–287. https://doi.org/10.1016/j.neuroimage.2015.02.063.

Raichle, M.E., 2015. The brain's default mode network. Annu. Rev. Neurosci. 38, 433–447. https://doi.org/10.1146/annurev-neuro-071013-014030.

Razoux, F., Baltes, C., Mueggler, T., Seuwen, A., Russig, H., Mansuy, I., Rudin, M., 2013. Functional MRI to assess alterations of functional networks in response to pharmacological or genetic manipulations of the serotonergic system in mice. Neuroimage 74, 326–336. https://doi.org/10.1016/j.neuroimage.2013.02.031.

Reig, R., Mattia, M., Compte, A., Belmonte, C., Sanchez-Vives, M.V., 2010. Temperature modulation of slow and fast cortical rhythms. J. Neurophysiol. 103, 1253–1261. https://doi.org/10.1152/jn.00890.2009.

Richiardi, J., Altmann, A., Milazzo, A.-C., Chang, C., Chakravarty, M.M., Banaschewski, T., Barker, G.J., Bokde, A.L.W., Bromberg, U., Büchel, C., Conrod, P., Fauth-Bühler, M., Flor, H., Frouin, V., Gallinat, J., Garavan, H., Gowland, P., Heinz, A., Lemaître, H., Mann, K.F., Martinot, J.-L., Nees, F., Paus, T., Pausova, Z., Rietschel, M., Robbins, T.W., Smolka, M.N., Spanagel, R., Ströhle, A., Schumann, G., Hawrylycz, M., Poline, J.-B., Greicius, M.D., IMAGEN consortium, 2015. Correlated gene expression supports synchronous activity in brain networks. Science 348, 1241–1244. https://doi.org/10.1126/science.1255905.

Roelofs, T.J.M., Verharen, J.P.H., van Tilborg, G.A.F., Boekhoudt, L., van der Toorn, A., de Jong, J.W., Luijendijk, M.C.M., Otte, W.M., Adan, R.A.H., Dijkhuizen, R.M., 2017. A novel approach to map induced activation of neuronal networks using chemogenetics and functional neuroimaging in rats: a proof-of-concept study on the mesocorticolimbic system. Neuroimage 156, 109–118. https://doi.org/10.1016/j.neuroimage.2017.05.021.

Sandi, C., Haller, J., 2015. Stress and the social brain: behavioural effects and neurobiological mechanisms. Nat. Rev. Neurosci. 16, 290–304. https://doi.org/10.1038/nrn3918.

Schroeter, A., Grandjean, J., Schlegel, F., Saab, B.J., Rudin, M., 2017. Contributions of structural connectivity and cerebrovascular parameters to functional magnetic resonance imaging signals in mice at rest and during sensory paw stimulation. J. Cereb. Blood Flow. Metab. 37, 2368–2382. https://doi.org/10.1177/0271678X16666292.

Schroeter, A., Schlegel, F., Seuwen, A., Grandjean, J., Rudin, M., 2014. Specificity of stimulus-evoked fMRI responses in the mouse: the influence of systemic physiological changes associated with innocuous stimulation under four different anesthetics. Neuroimage 94, 372–384. https://doi.org/10.1016/j.neuroimage.2014.01.046.

Schwarz, A.J., Gass, N., Sartorius, A., Risterucci, C., Spedding, M., Schenker, E., Meyer-Lindenberg, A., Weber-Fahr, W., 2013. Anti-correlated cortical networks of intrinsic connectivity in the rat brain. Brain Connect. 3, 503–511. https://doi.org/10.1089/brain.2013.0168.

Sekar, S., Jonckers, E., Verhoye, M., Willems, R., Veraart, J., Van Audekerke, J., Couto, J., Giugliano, M., Wuyts, K., Dedeurwaerdere, S., Sijbers, J., Mackie, C., Ver Donck, L., Steckler, T., Van der Linden, A., 2013. Subchronic memantine induced concurrent functional disconnectivity and altered ultra-structural tissue integrity in the rodent brain: revealed by multimodal MRI. Psychopharmacol. Berl. 227, 479–491. https://doi.org/10.1007/s00213-013-2966-3.

Seminowicz, D.A., Jiang, L., Ji, Y., Xu, S., Gullapalli, R.P., Masri, R., 2012. Thalamocortical asynchrony in conditions of spinal cord injury pain in rats. J. Neurosci. 32, 15843–15848. https://doi.org/10.1523/JNEUROSCI.2927-12.2012.

Sforazzini, F., Bertero, A., Dodero, L., David, G., Galbusera, A., Scattoni, M.L., Pasqualetti, M., Gozzi, A., 2014a. Altered functional connectivity networks in acallosal and socially impaired BTBR mice. Brain Struct. Funct. https://doi.org/10.1007/s00429-014-0948-9.

Sforazzini, F., Schwarz, A.J., Galbusera, A., Bifone, A., Gozzi, A., 2014b. Distributed BOLD and CBV-weighted resting-state networks in the mouse brain. Neuroimage 87, 403–415. https://doi.org/10.1016/j.neuroimage.2013.09.050.

Shah, D., Blockx, I., Guns, P., Paul, P., Deyn, D., Dam, D. Van, Jonckers, E., Delgado, R., Verhoye, M., Linden, A. Van Der, 2015. Acute modulation of the cholinergic system in the mouse brain detected by pharmacological resting-state functional MRI. Neuroimage 109, 151–159. https://doi.org/10.1016/j.neuroimage.2015.01.009.

Shah, D., Blockx, I., Keliris, G.A., Kara, F., Jonckers, E., Verhoye, M., Van der Linden, A., 2016a. Cholinergic and serotonergic modulations differentially affect large-scale functional networks in the mouse brain. Brain Struct. Funct. 221, 3067–3079. https://doi.org/10.1007/s00429-015-1087-7.

Shah, D., Deleye, S., Verhoye, M., Staelens, S., Van der Linden, A., 2016b. Resting-state functional MRI and [18F]-FDG PET demonstrate differences in neuronal activity between commonly used mouse strains. Neuroimage 125, 571–577. https://doi.org/10.1016/j.neuroimage.2015.10.073.

Shah, D., Jonckers, E., Praet, J., Vanhoutte, G., Delgado Y Palacios, R., Bigot, C., D'Souza, D.V., Verhoye, M., Van der Linden, A., 2013. Resting state FMRI reveals diminished functional connectivity in a mouse model of amyloidosis. PLoS One 8, e84241. https://doi.org/10.1371/journal.pone.0084241.

Shah, D., Praet, J., Latif Hernandez, A., Höfling, C., Anckaerts, C., Bard, F., Morawski, M., Detrez, J.R., Prinsen, E., Villa, A., De Vos, W.H., Maggi, A., D'Hooge, R., Balschun, D., Rossner, S., Verhoye, M., Van der Linden, A., 2016c. Early pathologic amyloid induces hypersynchrony of BOLD resting-state networks in transgenic mice and provides an early therapeutic window before amyloid plaque deposition. Alzheimers. Dement. 12, 964–976. https://doi.org/10.1016/j.jalz.2016.03.010.

Sharp, D.J., Scott, G., Leech, R., 2014. Network dysfunction after traumatic brain injury. Nat. Rev. Neurol. 10, 156–166. https://doi.org/10.1038/nrneurol.2014.15.

Shim, W.H., Suh, J.-Y., Kim, J.K., Jeong, J., Kim, Y.R., 2017. Enhanced thalamic functional connectivity with No fMRI responses to affected forelimb stimulation in stroke-recovered rats. Front. Neural Circuits 10, 1–11. https://doi.org/10.3389/fncir.2016.00113.

Shmueli, K., van Gelderen, P., de Zwart, J.A., Horovitz, S.G., Fukunaga, M., Jansma, J.M., Duyn, J.H., 2007. Low-frequency fluctuations in the cardiac rate as a source of variance in the resting-state fMRI BOLD signal. Neuroimage 38, 306–320. https://doi.org/10.1016/j.neuroimage.2007.07.037.

Stafford, J.M., Jarrett, B.R., Miranda-Dominguez, O., Mills, B.D., Cain, N., Mihalas, S., Lahvis, G.P., Lattal, K.M., Mitchell, S.H., David, S.V., Fryer, J.D., Nigg, J.T., Fair, D.A., 2014. Large-scale topology and the default mode network in the mouse connectome. Proc. Natl. Acad. Sci. 111, 18745–18750. https://doi.org/10.1073/pnas.1404346111.

Tambini, A., Ketz, N., Davachi, L., 2010. Enhanced brain correlations during rest are related to memory for recent experiences. Neuron 65, 280–290. https://doi.org/10.1016/j.neuron.2010.01.001.

Teipel, S.J., Bokde, A.L.W., Meindl, T., Amaro, E., Soldner, J., Reiser, M.F., Herpertz, S.C., Möller, H.-J., Hampel, H., 2010. White matter microstructure underlying default mode network connectivity in the human brain. Neuroimage 49, 2021–2032. https://doi.org/10.1016/j.neuroimage.2009.10.067.

Thompson, P.M., Ge, T., Glahn, D.C., Jahanshad, N., Nichols, T.E., 2013. Genetics of the connectome. Neuroimage 80, 475–488. https://doi.org/10.1016/j.neuroimage.2013.05.013.

Uchida, S., Bois, S., Guillemot, J.-P., Leblond, H., Piché, M., 2017. Systemic blood pressure alters cortical blood flow and neurovascular coupling during nociceptive processing in the primary somatosensory cortex of the rat. Neuroscience 343, 250–259. https://doi.org/10.1016/j.neuroscience.2016.12.014.

Ueki, M., Mies, G., Hossmann, K.A., 1992. Effect of alpha-chloralose, halothane, pentobarbital and nitrous oxide anesthesia on metabolic coupling in somatosensory cortex of rat. Acta Anaesthesiol. Scand. 36, 318–322.

Upadhyay, J., Baker, S.J., Chandran, P., Miller, L., Lee, Y., Marek, G.J., Sakoglu, U., Chin, C.L., Luo, F., Fox, G.B., Day, M., 2011. Default-mode-like network activation in awake rodents. PLoS One 6. https://doi.org/10.1371/journal.pone.0027839.

Urban, D.J., Roth, B.L., 2015. DREADDs (designer receptors exclusively activated by designer drugs): chemogenetic tools with therapeutic utility. Annu. Rev. Pharmacol. Toxicol. 55, 399–417. https://doi.org/10.1146/annurev-pharmtox-010814-124803.

Van Den Berge, N., Albaugh, D.L., Salzwedel, A., Vanhove, C., Van Holen, R., Gao, W., Stuber, G.D., Ian Shih, Y.-Y., 2017. Functional circuit mapping of striatal output nuclei using simultaneous deep brain stimulation and fMRI. Neuroimage 146, 1050–1061. https://doi.org/10.1016/j.neuroimage.2016.10.049.

van den Heuvel, M.P., Bullmore, E.T., Sporns, O., 2016. Comparative connectomics. Trends Cogn. Sci. 20, 345–361. https://doi.org/10.1016/j.tics.2016.03.001.

van der Marel, K., Homberg, J.R., Otte, W.M., Dijkhuizen, R.M., 2013. Functional and structural neural network characterization of serotonin transporter knockout rats. PLoS One 8, e57780. https://doi.org/10.1371/journal.pone.0057780.

van Meer, M., Otte, W.M., van der Marel, K., Nijboer, C.H., Kavelaars, A., van der Sprenkel, J.W.B., Viergever, M.A., Dijkhuizen, R.M., 2012. Extent of bilateral neuronal network reorganization and functional recovery in relation to stroke severity. J. Neurosci. 32, 4495–4507. https://doi.org/10.1523/JNEUROSCI.3662-11.2012.

van Meer, M.P.A., van der Marel, K., Otte, W.M., Berkelbach van der Sprenkel, J.W., Dijkhuizen, R.M., 2010a. Correspondence between altered functional and structural connectivity in the contralesional sensorimotor cortex after unilateral stroke in rats: a combined resting-state functional MRI and manganese-enhanced MRI study. J. Cereb. Blood Flow. Metab. 30, 1707–1711. https://doi.org/10.1038/jcbfm.2010.124.

van Meer, M.P.A., van der Marel, K., Wang, K., Otte, W.M., el Bouazati, S., Roeling, T.A.P., Viergever, M.A., Berkelbach van der Sprenkel, J.W., Dijkhuizen, R.M., 2010b. Recovery of sensorimotor function after experimental stroke correlates with restoration of resting-state interhemispheric functional connectivity. J. Neurosci. 30, 3964–3972. https://doi.org/10.1523/JNEUROSCI.5709-09.2010.

Vanhoutte, G., Verhoye, M., Van Der Linden, A., 2006. Changing body temperature affects the T2* signal in the rat brain and reveals hypothalamic activity. Magn. Reson. Med. 55, 1006–1012. https://doi.org/10.1002/mrm.20861.

Veer, I.M., Beckmann, C.F., van Tol, M.-J., Ferrarini, L., Milles, J., Veltman, D.J., Aleman, A., van Buchem, M.A., van der Wee, N.J., Rombouts, S.A.R.B., 2010. Whole brain resting-state analysis reveals decreased functional connectivity in major depression. Front. Syst. Neurosci. 4, 1–10. https://doi.org/10.3389/fnsys.2010.00041.

Vetere, G., Kenney, J.W., Tran, L.M., Xia, F., Steadman, P.E., Parkinson, J., Josselyn, S.A., Frankland, P.W., 2017. Chemogenetic interrogation of a brain-wide fear memory network in mice. Neuron 94, 363–374. https://doi.org/10.1016/j.neuron.2017.03.037 e4.

Wang, K., van Meer, M.P.A., van der Marel, K., van der Toorn, A., Xu, L., Liu, Y., Viergever, M.A., Jiang, T., Dijkhuizen, R.M., 2011. Temporal scaling properties and spatial synchronization of spontaneous blood oxygenation level-dependent (BOLD) signal fluctuations in rat sensorimotor network at different levels of isoflurane anesthesia. NMR Biomed. 24, 61–67. https://doi.org/10.1002/nbm.1556.

Wang, K., Zheng, C., Wu, C., Gao, M., Liu, Q., Yang, K., Ellsworth, K., Xu, L., Wu, J., 2008. alpha-Chloralose diminishes gamma oscillations in rat hippocampal slices. Neurosci. Lett. 441, 66–71. https://doi.org/10.1016/j.neulet.2008.06.014.

Wang, R., Foniok, T., Wamsteeker, J.I., Qiao, M., Tomanek, B., Vivanco, R.A., Tuor, U.I., 2006. Transient blood pressure changes affect the functional magnetic resonance imaging detection of cerebral activation. Neuroimage 31, 1–11. https://doi.org/10.1016/j.neuroimage.2005.12.004.

Weber, R., Ramos-Cabrer, P., Wiedermann, D., van Camp, N., Hoehn, M., 2006. A fully noninvasive and robust experimental protocol for longitudinal fMRI studies in the rat. Neuroimage 29, 1303–1310. https://doi.org/10.1016/j.neuroimage.2005.08.028.

White, B.R., Bauer, A.Q., Snyder, A.Z., Schlaggar, B.L., Lee, J.-M., Culver, J.P., 2011. Imaging of functional connectivity in the mouse brain. PLoS One 6, e16322. https://doi.org/10.1371/journal.pone.0016322.

Wiggins, J.L., Bedoyan, J.K., Peltier, S.J., Ashinoff, S., Carrasco, M., Weng, S.-J., Welsh, R.C., Martin, D.M., Monk, C.S., 2012. The impact of serotonin transporter (5-HTTLPR) genotype on the development of resting-state functional connectivity in children and adolescents: a preliminary report. Neuroimage 59, 2760–2770. https://doi.org/10.1016/j.neuroimage.2011.10.030.

Williams, K.A., Magnuson, M., Majeed, W., LaConte, S.M., Peltier, S.J., Hu, X., Keilholz, S.D., 2010. Comparison of alpha-chloralose, medetomidine and isoflurane anesthesia for functional connectivity mapping in the rat. Magn. Reson. Imaging 28, 995–1003. https://doi.org/10.1016/j.mri.2010.03.007.

Williams, K.A., Mehta, N.S., Redei, E.E., Wang, L., Procissi, D., 2014. Aberrant resting-state functional connectivity in a genetic rat model of depression. Psychiatry Res. 222, 1–3. https://doi.org/10.1016/j.pscychresns.2014.02.001.

Wilson, D.A., Hoptman, M.J., Gerum, S.V., Guilfoyle, D.N., 2011. State-dependent functional connectivity of rat olfactory system assessed by fMRI. Neurosci. Lett. 497, 69–73. https://doi.org/10.1016/j.neulet.2011.04.031.

Wise, R.A., 2004. Dopamine, learning and motivation. Nat. Rev. Neurosci. 5, 483–494. https://doi.org/10.1038/nrn1406.

Yeo, B.T.T., Krienen, F.M., Sepulcre, J., Sabuncu, M.R., Lashkari, D., Hollinshead, M., Roffman, J.L., Smoller, J.W., Zöllei, L., Polimeni, J.R., Fischl, B., Liu, H., Buckner, R.L., 2011. The organization of the human cerebral cortex estimated by intrinsic functional connectivity. J. Neurophysiol. 106, 1125–1165. https://doi.org/10.1152/jn.00338.2011.

Zeng, L.L., Shen, H., Liu, L., Wang, L., Li, B., Fang, P., Zhou, Z., Li, Y., Hu, D., 2012. Identifying major depression using whole-brain functional connectivity: a multivariate pattern analysis. Brain 135, 1498–1507. https://doi.org/10.1093/brain/aws059.

Zerbi, V., Grandjean, J., Rudin, M., Wenderoth, N., 2015. Mapping the mouse brain with rs-fMRI: an optimized pipeline for functional network identification. Neuroimage 123, 11–21. https://doi.org/10.1016/j.neuroimage.2015.07.090.

Zerbi, V., Wiesmann, M., Emmerzaal, T.L., Jansen, D., Van Beek, M., Mutsaers, M.P.C., Beckmann, C.F., Heerschap, A., Kiliaan, A.J., 2014. Resting-state functional connectivity changes in aging apoE4 and apoe-KO mice. J. Neurosci. 34, 13963–13975. https://doi.org/10.1523/JNEUROSCI.0684-14.2014.

Zhan, Y., Paolicelli, R.C., Sforazzini, F., Weinhard, L., Bolasco, G., Pagani, F., Vyssotski, A.L., Bifone, A., Gozzi, A., Ragozzino, D., Gross, C.T., 2014. Deficient neuron-microglia signaling results in impaired functional brain connectivity and social behavior. Nat. Neurosci. 17, 400–406. https://doi.org/10.1038/nn.3641.

Zhang, F., Aravanis, A.M., Adamantidis, A., de Lecea, L., Deisseroth, K., 2007. Circuit-breakers: optical technologies for probing neural signals and systems. Nat. Rev. Neurosci. 8, 577–581. https://doi.org/10.1038/nrn2192.

Zhao, F., Zhao, T., Zhou, L., Wu, Q., Hu, X., 2008. BOLD study of stimulation-induced neural activity and resting-state connectivity in medetomidine-sedated rat. Neuroimage 39, 248–260. https://doi.org/10.1016/j.neuroimage.2007.07.063.

Zhou, I.Y., Liang, Y., Chan, R.W., Gao, P.P., Cheng, J.S., Hu, Y., So, K., Wu, E.X., 2014. Brain resting-state functional MRI connectivity: morphological foundation and plasticity. Neuroimage 84, 1–10. https://doi.org/10.1016/j.neuroimage.2013.08.037.

Zhurakovskaya, E., Paasonen, J., Shatillo, A., Lipponen, A., Salo, R., Aliev, R., Tanila, H., Gröhn, O., 2016. Global functional connectivity differences between sleep-like states in urethane anesthetized rats measured by fMRI. PLoS One 11, e0155343. https://doi.org/10.1371/journal.pone.0155343.

Zingg, B., Hintiryan, H., Gou, L., Song, M.Y., Bay, M., Bienkowski, M.S., Foster, N.N., Yamashita, S., Bowman, I., Toga, A.W., Dong, H.W., 2014. Neural networks of the mouse neocortex. Cell 156, 1096–1111. https://doi.org/10.1016/j.cell.2014.02.023.